Cloud Responses to Abrupt Solar and CO_2 Forcing Part II: Adjustment to Forcing in Coupled Models

Enter authors here: T. Aerenson[1], R. Marchand[1], C. Zhou[2]

[1]University of Washington Department of Atmospheric Sciences, Seattle, WA, USA. [2]School of Atmospheric Sciences, Nanjing University, Nanjing, China.

Corresponding author: Travis Aerenson (aerenson@uw.edu)

Key Points:

- Increasing CO_2 causes a reduction, and lowering of mid-level and low-level clouds which does not occur from solar forcing.
- There is large reduction in optically thin high clouds in solp4p, especially as compared with 4xCO2.
- Even after 150 years adjustments make a significant contribution to the total net cloud radiative effect.

Abstract

In this paper we examine differences in cloud adjustments (often called rapid adjustments) that occur as a direct result of abruptly increasing the solar constant by 4% or abruptly quadrupling of atmospheric CO_2. In doing so, we devised a novel method for calculating the cloud adjustments for the abrupt solar forcing experiment that uses differences between coupled model simulations with abrupt solar and CO_2 forcing, in combination with uncoupled, atmosphere-only, abrupt CO_2 forced experiments that have prescribed sea-surface temperature. Our main findings are that 1) there are substantial differences in the response of stratocumulus and cumulus clouds to solar and CO_2 forcing, which follow the differences in the direct radiative effect that solar and CO_2 forcing have at cloud top, and 2) there are differences in the adjustment of the average optical depth of high clouds to solar and CO_2 forcing that we speculate are driven by the differences in the vertical profile of radiative heating, and differences in the pattern of sea-surface temperature change (for a fixed global mean temperature). Such adjustments do contribute significantly to the total net cloud radiative effect, even after 150 years of simulation.

Plain Language Summary

In climate change, clouds change due to a variety of mechanisms including surface temperature, dynamical circulations, and radiative forcing. In this paper we examine the latter: how clouds respond to radiative forcing. We study this topic using climate model simulations where the brightness of the sun is abruptly increased by 4% and compare those with simulations where CO_2 concentration is abruptly quadrupled. In doing so we find that there are differences in the cloud response to changes in solar and CO_2 forcing which include the occurrence of thick and thin high cloud, as well as the amount and height of low and mid-level clouds.

1. Introduction

The climate is changing due to anthropogenic emissions of heat-trapping gasses, and our ability to predict the amount of surface warming that will occur depends critically on knowing how cloud optical depth, cloud-top height and cloud amount will change (Sherwood et al., 2020; Zelinka et al., 2020). How clouds will change can be decomposed into the sum of two components, a surface-temperature mediated change (the cloud change that is a function of global mean temperature anomaly and sea-surface temperature and sea ice change pattern) and a cloud adjustment that occurs directly due to the forcing agent, in our case from changes in insolation or atmospheric CO_2 concentration (Sherwood et al., 2015). In this paper we focus on the cloud adjustments, while in a companion paper (Aerenson & Marchand, 2023; hereafter Part I), we focus on the temperature mediated component.

As detailed in Part I, we analyze cloud feedbacks in model simulations produced as a part of the third phase of the Cloud Feedback Model Intercomparison Project (CFMIP3; Webb et al.,

2017) which is a part of the sixth phase of the Coupled Model Intercomparison Project (CMIP6). Specifically, in CFMIP3 a pair of model simulations were performed in fully coupled climate models initialized from the pre-industrial climate, and then perturbed by suddenly increasing or decreasing the insolation by 4% (hereafter solp4p and solm4p experiments respectively). In this paper, and Part I, we compare and contrast these two abrupt-solar experiments with simulations in which there is an abrupt quadrupling of the CO_2 concentration (hereafter 4xCO2) and halving of CO_2 (hereafter 0p5xCO2) that were also produced as a part of the CMIP6 experiments (Eyring et al., 2016). We also use experiments from the Atmospheric Model Intercomparison Project (hereafter AMIP), in which atmosphere-only model configurations are run with the sea-surface temperatures prescribed to match reanalysis (Gates et al., 1999). Specifically, we use simulations where the atmospheric CO_2 is quadrupled without allowing for the sea-surface temperatures or sea-ice to adjust to the forcing. These simulations nominally allow us to estimate the adjustment that occurs directly from CO_2 increase independent of sea-surface temperature increase. There are however limitations to this method, in that the land temperature is allowed to warm, which introduces land-ocean temperature gradients (and associated monsoonal circulations) to the model simulation, which are not in-fact a direct response of the atmosphere to the forcing mechanism (Andrews et al., 2021a). In addition to the CMIP6 experiments, we use independently performed model simulations of the solp4p and 4xCO2 experiments from both coupled and atmosphere-only (AMIP-style) model integrations of CESM1, as well as simulations from CMIP5 generation models with 2xCO2 and a 2% increase of the solar constant in both the fully coupled and atmosphere-only (AMIP style) model configurations. These later simulations serve as a testbed for the method we have developed to calculate the adjustment to solar forcing, without atmosphere-only integrations of solp4p from the CMIP6 models, which is described in detail in Section 2 of this paper.

Through this analysis we seek to understand how cloud adjustments caused by solar and CO_2 forcing differ, and the underlying physical mechanisms. Adjustments to CO_2 increase have been studied with a hierarchy of model simulations (e.g. Larson & Portmann, 2016; Schneider et al., 2019; Zelinka et al., 2013), and there are also a few previous studies which examine abrupt changes in solar forcing, and the differences in adjustments to different forcing agents. Smith et al. (2018) studied the adjustment to various forcing agents (including increasing the solar constant by 2% and doubling CO_2) using atmosphere only integrations of an ensemble of climate models (similar to the model configurations of the AMIP simulations). This allowed them to diagnose the adjustments from the various forcing changes. They found that the global mean adjustment of top-of-atmosphere radiation that results from cloud adjustments to solar forcing is of opposite sign from the cloud adjustment to CO_2 forcing. That is, after an increase in CO_2, cloud adjustments created a positive (warming) radiative forcing while increasing the solar constant produced a cloud response that contributed a negative (cooling) radiative forcing. Because of this difference in cloud adjustments, the top-of-atmosphere radiation imbalance is greater following CO_2 forcing than solar forcing. In our analysis, using a different method to diagnose cloud radiative effect, we find that the radiative adjustments to cloud following CO_2 and solar forcing are both positive (warming effect on the climate), however the adjustment is greater following the CO_2 forcing. We discuss this difference further in Section 4 of this article.

Salvi et al. (2021) similarly studied the adjustment to various forcing agents in a model with prescribed sea-surface temperature and sea-ice. They used offline radiative transfer calculations to find the expected change in the vertical profiles of radiative heating anomaly from each forcing agent and found that there were differences in the adjustment to solar and CO_2 forcing due to the radiative effect of CO_2 forcing being largest in the lower troposphere, while the radiative impact of solar forcing is nearly vertically uniform throughout the troposphere. Although it was not explicitly shown by Salvi et al. (2021), one expects the differences in the heating rate of the upper troposphere to impact the formation and lifetime of high clouds (Dinh et al., 2010; Gasparini et al., 2019; Seeley et al., 2019), as well as the static stability of the lower troposphere.

There are also adjustments to CO_2 and solar forcing over land which have received some attention. Evapotranspiration is an important moisture source over land, and the associated evaporative cooling is important for setting the climatological land temperature. Upon CO_2 increase, plant stomata do not open as wide, which reduces evapotranspiration rates (e.g. Betts et al., 1997; Cox et al., 1999; Field et al., 1995). In contrast, upon solar forcing increase one expects the increase in total SW radiation reaching the surface to increase photosynthesis (and evapotranspiration) rates (Mercado et al., 2009). In a comparison of experiments with CO_2 doubling and solar constant increase of 2.25% where the plant physiological effects of CO_2 are isolated from the radiative effects on the atmosphere Modak et al. (2016) found that the effect of CO_2 on evapotranspiration increases land surface warming on as short of timescales as 7-days following forcing (when little sea-surface temperature change has occurred). They find that the reduced evapotranspiration rate from CO_2 forcing causes less cloud occurrence over land after CO_2 forcing compared with solar forcing.

Additionally, there has been work done studying the effects of simultaneous solar and CO_2 forcing by Russotto & Ackerman (2018), who analyzed cloud changes in the Geoengineering Model Intercomparison Project (GeoMIP) G1 experiment, in which the CO_2 concentration is abruptly quadrupled while simultaneously the solar constant is decreased by an amount tuned so that the top-of-atmosphere radiation budget of each participating model has zero net radiative forcing (Kravitz et al., 2015). This required a decrease in the solar constant between 3.2% and 5.0% depending on the model. Russotto & Ackerman 2018 found that the immediate adjustments of clouds following the abrupt forcing was a vital component to determining how much solar forcing is required to balance the CO_2 forcing in each model. They found numerous cloud changes in the G1 experiment that contribute to the top-of-atmosphere radiation balance, such as a reduction of stratocumulus clouds associated with a decrease in inversion strength, and an increase of high clouds along the ITCZ and SPCZ. They did however recognize that understanding the underlying physical mechanisms responsible for the cloud changes would require simulations that perturb the CO_2 concentration and solar constant independently, as we do here.

This paper is organized as follows: Section 2 contains a description of the model data, and methods used in this study, including a description of the method we use to calculate adjustment from coupled model simulations, and how we relate cloud changes to radiative flux using cloud radiative kernels. Then in Section 3 we present the results which includes the cloud adjustment to solp4p and 4xCO2, the impact the cloud changes have on top-of-atmosphere radiative flux, and additional results which help interpret the physical mechanisms responsible for the *adjustment difference* between solp4p and 4xCO2. The results are discussed in the broader context of the existing literature in Section 4, and the main conclusions of this paper, and Part I are synthesized in Section 5.

2. Data and Methods

2.1 Model Experiments

In CMIP6 a total of five modeling centers performed the solp4p and 4xCO2 experiments, as well as the AMIP experiment with abrupt quadrupling of CO_2 (hereafter referred to as AMIP-4xCO2). Details on the CMIP6 models are available in Part I.

Additionally, we use a set of independently performed simulations with the Community Earth System Model 1.2.1 Community Atmosphere Model 5.3 (hereafter referred to as CESM1) run at 1.9° latitude x 2.5° longitude resolution (Neale et al., 2012). From these simulations we have results of both the 4xCO2 and solp4p experiments, using both the fully coupled and atmosphere only (AMIP-style) simulations with prescribed sea-surface temperature and sea-ice. The addition of AMIP-style runs with solar and CO_2 forcing allow us to compare several techniques to calculate the cloud adjustments from the fully coupled CMIP6 solp4p simulations. In this independent set of CESM1 simulations there are 3 ensemble members of the 4xCO2 experiments, and single simulations for the other experiments. Data from these simulations were first published by Zhou et al. (2023) and are available for download at https://doi.org/10.5281/zenodo.7193943.

Lastly, we use output from model experiments that were requested for the Precipitation Drivers Response Model Intercomparison Project (PDRMIP), in which there are simulations of 2xCO2, and solp2p (abrupt doubling of CO_2 and 2% increase of the solar constant respectively) that were performed in both the fully coupled, and fixed sea-surface temperature and sea ice configurations. We also use these PDRMIP experiments as a testbed for the method we ultimately use to estimate the adjustment from the solp4p in the CMIP6 coupled model simulations. However, these experiments do not include the ISCCP satellite simulator outputs. A full description of the PDRMIP data is provided by Andrews et al. (2021b) and Myhre et al. (2022), and these data are available at https://cicero.oslo.no/en/projects/pdrmip/pdrmip-data-access.

2.2 Methods and Theory of Adjustment Calculation

When an abrupt forcing is imposed on the climate, the cloud changes are often decomposed into two components: those driven by changes in global mean surface temperature (which are called temperature mediated change), and those that are independent of the global mean surface temperature (which are called the adjustments), as described by Equation 1, where $C(\theta, \phi, t)$ represents the cloud amount anomaly at a given latitude, longitude, and time in the simulation, $A(\theta, \phi)$ is the adjustment to the forcing change at a certain latitude and longitude, $\Delta T(t)$ is the global mean surface temperature anomaly at a given time, $M(\theta, \phi, \Delta T(t))$ is the temperature mediated component, and $\varepsilon(t)$ represents internal variability which causes cloud changes which are due to neither the global mean temperature change or adjustments. In this paper, we are concerned with calculating the adjustment term $A(\theta, \phi)$.

$$C(\theta, \phi, t) = A(\theta, \phi) + M\big(\theta, \phi, \Delta T(t)\big) + \varepsilon(t) \qquad (1)$$

The temperature mediated changes are often approximated by a linear relationship to global mean surface temperature, such that M can be written as $M\big(\theta, \phi, \Delta T(t)\big) \approx M(\theta, \phi)\Delta T(t)$ (e.g. Ceppi et al., 2017; Gregory et al., 2004; Zelinka et al., 2013) as is done in Part I, and ideally $A(\theta, \phi)$ is simply the intercept that is found by fitting a line to the simulated cloud anomaly as a function of ΔT. However, in truth this system is not completely linear, and for example, cloud amount depends on not-only the global mean temperature, but also the surface temperature pattern and associated dynamical circulations (Andrews et al., 2015, 2022; Williams et al., 2008). Although the linear model fits the total global mean cloud response well after the first couple decades following the abrupt forcing there can be large deviations from linearity (especially at the local grid-cell level) which make it problematic to obtain $A(\theta, \phi)$ as the intercept, or to interpret the intercept as the true adjustment (for discussion of this subject see **Supplemental Materials**).

We are not the first to recognize this problem, and to avoid reliance on a linear model, as well as to avoid errors that might result from internal variability (especially with variability on longer-than-annual timescales), the adjustment has often been calculated using model experiments that impose an abrupt forcing with sea-surface temperatures (SST) prescribed to match reanalysis such that the atmospheric adjustment is isolated from the effects of SST change, hereafter referred to as fixed-SST experiments (e.g. Colman & McAvaney, 2011; Forster et al., 2016; Gregory & Webb, 2008; Smith et al., 2018; Zelinka et al., 2013). Specifically, the adjustment term is calculated as the difference in cloud amount or radiative effect between fixed-SST experiment with and without the addition of forcing (i.e. AMIP-4xCO2 minus AMIP) over periods long enough to make the effect of internal variability small, typically 20-30 years.

As was noted in Section 1, this fixed-SST approach is not perfect because the land-surface is allowed to warm, which likely changes clouds over land, but also creates land-sea temperature contrasts that change atmospheric circulation patterns. Andrews et al. (2021a) compared the adjustments using fixed-SST experiments to those calculated in model experiments where all surface temperature is held constant during CO_2 quadrupling to understand the effect that land warming has on adjustment calculations. The impact of the fixed-SST approach on our results are discussed in Section 4.4.

At a practical level, our set of CMIP6 simulations of the solp4p experiment, contains no fixed-SST version, hence we derive a new method of calculating the adjustment to solp4p using a combination of coupled simulations of 4xCO2 and solp4p with the AMIP-4xCO2. To test our method, we use fixed-SST and coupled solp4p simulations from CESM1 as well as model simulations from the Precipitation Drivers Response Model Intercomparison Project (PDRMIP; Myhre et al., 2017) as described in the previous section. The first step in our new method is to calculate the difference in cloud amount (and/or cloud radiative effect) from the long-term average (years 10 to 150 following abrupt forcing) between the 4xCO2 and solp4p coupled model simulations, following Equation 2. Using a long climatology (such as 140 years) diminishes the impact of internal variability on the calculation. Hereafter we refer to this quantity ($\Delta A_{sol-CO2}(\theta,\phi)$) as the *adjustment difference*.

$$\Delta A_{sol-CO2}(\theta,\phi) = \langle C_{sol}(\theta,\phi,t)\rangle_{t=10-150} - \langle C_{CO2}(\theta,\phi,t)\rangle_{t=10-150} \tag{2}$$

Then, to estimate the adjustment solely due to solp4p, we simply add the adjustment to 4xCO2 (calculated as the difference between the AMIP-4xCO2 experiment and AMIP experiment) to the *adjustment difference*, as shown in Equation 3. Hereafter, we will refer to this as the solp4p *estimated adjustment* or simply the solp4p *adjustment*.

$$A_{sol}(\theta,\phi) = \Delta A_{sol-CO2}(\theta,\phi) + A_{CO2}(\theta,\phi) \tag{3}$$

To demonstrate the effectiveness of Equation 3 in capturing the adjustment to solp4p **Figure 1** shows the *estimated adjustment* of cloud amount to solp4p derived with Equation 3, and the fixed-SST derived adjustment of total cloud amount in CESM1 (top row), as well as cloud radiative effect (derived from top-of-atmosphere fluxes) adjustment in the solp2p experiments from both methods applied to the PDRMIP multi-model mean (lower three rows). We stress that the solp2p results from PDRMIP are not comparable to the solp4p experiment, and is only used here to validate the *estimated adjustment* method. Comparing the panels in the left column of **Figure 1**, which are based on Equation 3 with the right column that are based on AMIP-style experiments demonstrates that the *estimated adjustment* obtained via Equation 3 captures many of the patterns which occur in the AMIP-derived adjustment. For example, in the CESM1 simulations, there is a reduction of cloud amount over the Indian Ocean, and Tropical Pacific, which is consistent across the two methods. Additionally, there is a decrease in cloud amount over North America, and an increase in cloud amount over Amazonia, Africa, and Southeast Asia. Likewise, the *estimated adjustment* is in good agreement with the fixed-SST derived adjustment in for the PDRMIP solp2p experiments (consisting of eight participating models).

Ultimately, we find Equation 3 to be superior to several other approaches that we tested for estimating the solp4p adjustment, details on which can be found in the **Supplemental Materials**. On a minor note, we do of course find that the *adjustment difference* between the 4xCO2 and solp4p in the coupled model simulations produces a difference pattern that is remarkably consistent with the difference in adjustment calculated using the fixed-SST simulations. These results are also provided in the **Supplemental Materials**.

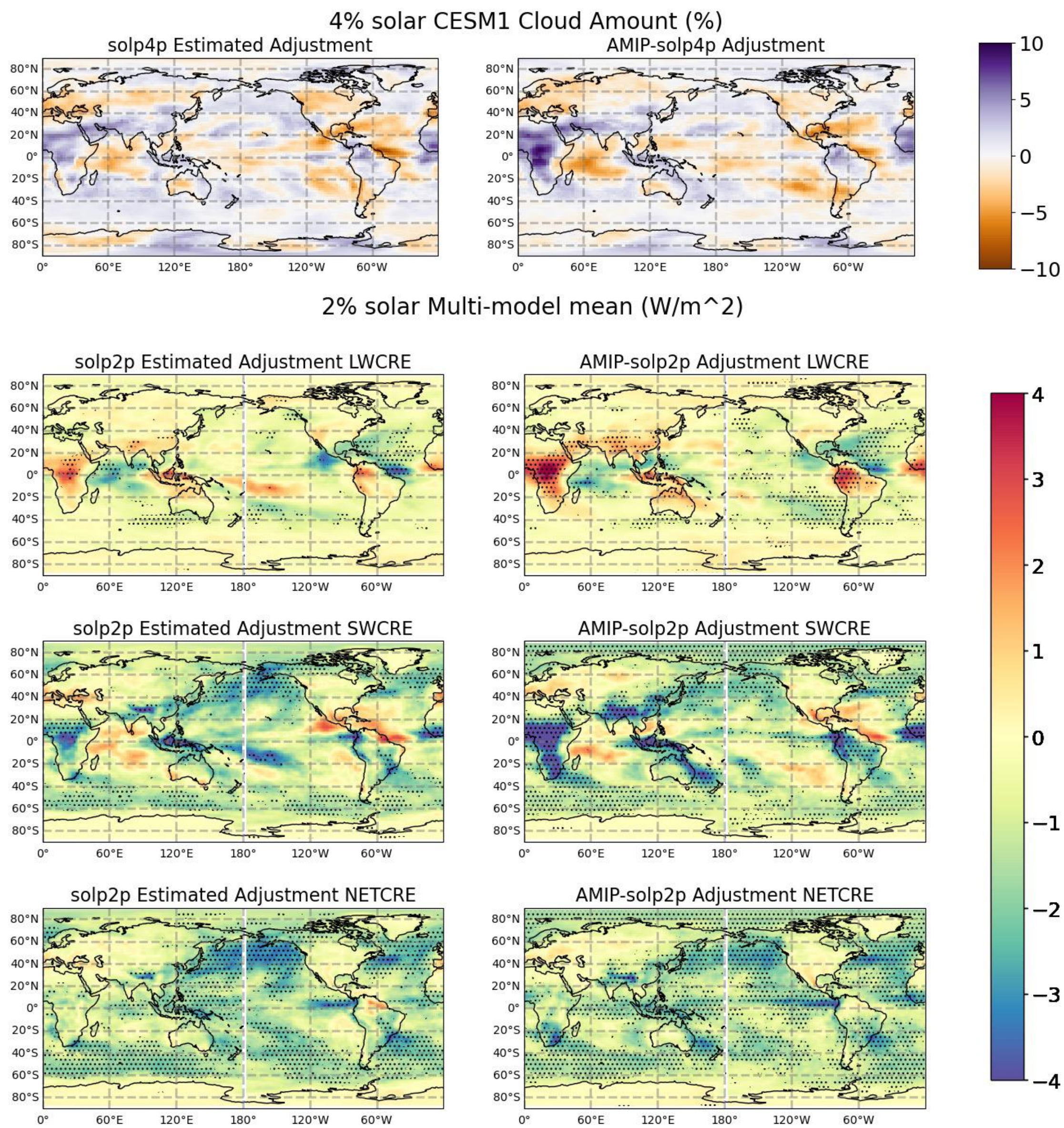

***Figure 1** Top row: Estimated adjustment (following Equation 3, lefthand figure) and AMIP-solp4p adjustment (righthand figure) of total cloud amount from CESM1 simulations Note that we use the ensemble mean of the three available 4xCO2 simulations of CESM1, the inter-realization variability is discussed in the Supplemental Materials. Bottom three rows: Estimated adjustment to 2% increase of solar constant (solp2p), and AMIP-solp2p adjustment of longwave,*

shortwave, and net cloud radiative effect. Stippling indicates regions where at least 6/8 models agree on the sign of the adjustment.

It is worth noting that this approach is not without its limitations. Firstly, it hinges upon the global mean temperature change being nearly equal in the solp4p and 4xCO2 experiments. If the temperature difference were large, then there would be considerable temperature mediated changes aliased with the *adjustment difference* such that it would be quite difficult to untangle the two. In the **Supplemental Materials** we calculate the *adjustment difference* between simulations with an abrupt reduction of the solar constant by 4% and an abrupt halving of atmospheric CO_2 (referred to as solm4p and 0p5xCO2 respectively). Details on these simulations are available in Part I. The solm4p and 0p5xCO2 are conceptually similar to the solp4p and 4xCO2, except that the imposed forcing has a cooling effect. However, there is roughly two times more cooling in the solm4p than the 0p5xCO2 simulations. We do not have fixed-SST versions of these simulations, so we cannot test if our new method works for these simulations, however upon inspection it is apparent that many of the patterns seen in the *adjustment difference* between solm4p and 0p5xCO2 are in fact due to the temperature mediated changes.

Secondly, even the *adjustment differences* calculated from our method are not entirely independent of SST change, because although the global mean temperature response in solp4p and 4xCO2 are quite similar, there is some difference in the warming pattern. We will see some *adjustment differences* in cloud that are likely due to differences in SST patterns in the solp4p and 4xCO2 adjustments. We consider this an important nuance of our method because this makes our method conceptually somewhat different from fixed-SST methods where the SST pattern is not allowed to change.

In the following sections both the *adjustment difference* and the *estimated adjustment* to solar forcing are presented. Each metric has its own utility, as the *adjustment difference* highlights the ways in which the cloud responses to the two forcing mechanisms differ, while the solp4p *estimated adjustment* shows how clouds change only because of increase in the solar constant.

2.3 ISCCP simulator and Cloud Radiative Kernels

To perform a comparison of cloud changes across models we make extensive use of the International Satellite Cloud Climatology Project (ISCCP) satellite simulator, which is part of the CFMIP Observation Simulator Package (COSP) and has been embedded into many climate models (Bodas-Salcedo et al., 2011). The ISCCP simulator is designed to imitate the results of ISCCP retrievals of cloud-top-pressure (CTP) and cloud optical depth based on visible and infrared images collected by geostationary weather satellites. The actual observational data have been collected into an ongoing global cloud datasets that has been operational since 1983 (Rossow & Schiffer, 1991). The ISCCP simulator parses total cloud fraction into CTP and cloud optical depth joint histograms, just as the ISCCP retrieval algorithm does. This allows for comparison of model clouds with observations, but also a comparison between models that is independent of each models' internal definition of "cloudiness".

Zelinka et al. (2012a) calculated cloud radiative kernels to compute longwave (hereafter LW) and shortwave (hereafter SW) top-of-atmosphere radiative fluxes associated with cloud effects from the ISCCP histograms. Using the radiative kernels, Zelinka et al., (2013) have examined cloud adjustment and temperature mediated response to 4xCO2 simulations from a collection of CMIP5 models. Here we undertake a similar analysis of the adjustment to solar and CO_2 forcing, and in order to understand the radiative impact that changes of cloud cover fraction (CF), cloud-top-height (CTH), and cloud optical depth (τ) have on top-of-atmosphere radiation balance, we perform a decomposition of the kernel-derived radiative effect into the radiative anomalies caused various cloud changes (as well as a small residual), following the method of Zelinka et al. (2012b) and Zelinka et al. (2013).

3. <u>Results</u>

In this section we present the results showing how cloud properties adjust to solar and CO_2 forcing and briefly examine the cloud radiative effect the adjustments have on top-of-atmosphere radiation using cloud radiative kernels. In Section 4 we discuss the physical mechanisms that likely contribute to the adjustments, and as a prelude to that discussion we close this section with an examination of changes in several other atmosphere and surface variables (such as 500 hPa vertical velocity, and estimated inversion strength).

3.1 <u>Adjustment of Cloud Properties to Solar and CO_2 Forcing</u>

Figures 2 and 3 show the *adjustment difference*, and the adjustment to quadrupling CO_2 calculated from the AMIP-4xCO2 experiment (top nine panels of **Figure 3**), and the *estimated adjustment* to solp4p calculated following the approach described in Section 2.2 (lower nine panels of **Figure 3**). Following Zelinka et al. (2013), we calculated the 4xCO2 rapid adjustment as the anomaly in cloud amount of each category averaged over the duration of the simulations, from years 5 to 36, using fixed SST simulations; and the *estimated adjustment* to solp4p is calculated following Equation 3. We separate the cloud changes into nine categories of Cloud Top Pressure (CTP) and optical depth. Specifically the cloud optical depth is broken into three ranges: optically thin ($\tau \leq 3.6$), optically medium ($3.6 < \tau \leq 23$), and optically thick ($\tau > 23$) clouds, and the CTP is likewise broken into three CTP ranges: low ($\mathrm{CTP} \geq 680$ hPa), mid-level (680 hPa $> \mathrm{CTP} \geq 440$ hPa), and high ($\mathrm{CTP} < 440$ hPa) cloud. We show the cloud changes as a multi-model mean, where stippling indicates regions where at least three out of four participating models agree on the sign of the cloud adjustment. Results from individual models are available in the **Supplemental Materials**. The 4xCO2 adjustments shown here are directly comparable to the results of Zelinka et al. (2013), and any differences are due primarily to differences between the set of CMIP5 models used by Zelinka et al. (2013) and the CMIP6 models used here (with a small contribution from internal variability). In the following paragraphs we describe the high, mid-level, and low cloud changes in sequence.

High Clouds:

The top row of **Figure 2** shows the *adjustment difference* of high clouds, where it is apparent that in most areas and in the global mean, there is less optically thin high cloud in the solp4p than the 4xCO2 adjustment (orange color) and more optically thick high cloud (purple color). The reduction in optically thin clouds is greater than the increase in optically medium and optically thick clouds such that there is less total high cloud in the solp4p experiment (Note: *adjustment differences* summed across all optical depth ranges are shown in **Supplemental Materials**).

For optically thin high cloud the *adjustment difference* (**Figure 2**) is greatest in the Tropics, especially over the Indian Ocean, Tropical West Pacific, and along the Pacific and Atlantic ITCZ. This difference in optically thin high cloud occurs across all individual models (see **Supplemental Materials** for individual model results). In **Figure 3** we can see that this difference is largely due to a stronger reduction of optically thin-high cloud in the solp4p *estimated adjustment*. In the AMIP-4xCO2 adjustment there is an increase in global mean cloud in this category, with noteworthy increases over the Central Pacific and over Africa. There is reduction in the 4xCO2 adjustment Indian and Atlantic Oceans, South America, and the Eastern Pacific, but in all of these regions the reduction in solp4p *estimated adjustment* is much greater, and in general, there are very few regions where the solp4p *estimated adjustment* shows an increase in optically thin high cloud.

For optically thick high cloud, the *adjustment difference* (**Figure 2**) is greatest in the Tropical West Pacific, but there is also more optically thick high cloud (purple color) and good model agreement (stippling) in other regions, including over the Eastern Indian Ocean, and several midlatitude locations (especially along the Southern Ocean storm track between 40° and 60° S). In the Eastern Equatorial Pacific, and a part of the Equatorial Atlantic, there is more optically thick high cloud in the 4xCO2 than solp4p (orange color), although there is poor model agreement as regards this feature. The overall adjustments in optically thick high clouds for the individual solp4p and 4xCO2 adjustments (**Figure 3**) are similar. In the Tropical West Pacific and Indian Ocean, where the optically thick high cloud *adjustment difference* is greatest, both the 4xCO2 adjustment and solp4p *estimated adjustment* show a decrease in optically thick high cloud. So, both forcing mechanisms cause a decrease of cloud in this category, but the change is greater from CO_2 than solar forcing. Likewise, in the midlatitudes, both adjustments show a reduction of optically thick high cloud over much of the midlatitudes. Thus, we again find that the greatest *adjustment difference* occurs when both experiments yield a decline in cloud occurrence, but there is greater decrease of optically thick high cloud in 4xCO2 than solp4p.

For optically medium high clouds, the *adjustment difference* (**Figure 2**) has fewer regions with good model agreement than the optically thin or thick high cloud categories. However, there is notably less cloud in this category in the solp4p than the 4xCO2 (orange color) in a small handful of regions including over the Indian Ocean, Atlantic ITCZ, Eastern Pacific portion of the ITCZ, Gulf Stream, and Kuroshio current. All of these regions have relatively warm SST (compared with surrounding regions), and are locations where convergence is common. As was the case for high-thick clouds, the overall pattern of adjustments in optically medium clouds for the individual solp4p and 4xCO2 adjustments (**Figure 3**) are similar, but in this case, it is the reduction in solp4p that is generally larger and results in a negative *adjustment difference* in the Indian and Atlantic Oceans. Over the Kuroshio current, near the coast of Japan there is poor model agreement on the individual adjustment terms, and this is one of the few places where the *adjustment difference* appears to be more robust than the individual adjustment terms.

Mid-Level Clouds:

Perhaps the most striking *adjustment difference* occurs in the mid-level cloud category (middle row of **Figure 2**), where there is positive difference (blue colors) in all optical thickness categories. This positive difference is widespread throughout the subtropics, midlatitudes and in the arctic. This difference is especially strong at medium optical depths, and in regions occupied by extensive stratocumulus off the western boundaries of continents. In the global mean (mean values are listed at the top of each panel), the *adjustment difference* is strongly positive in all three mid-level categories, with the change in thin cloud being stronger at higher latitudes. Looking at the *estimated adjustments* for the individual forcings (**Figure 3**), we see that in all three optical depth categories there is a substantial reduction in mid-level clouds associated with 4xCO2, that is especially strong in the stratocumulus regions, while the solp4p *estimated adjustment* shows an increase in the mid-level cloud over most oceans (and only weak decreases over land with little model agreement).

Low-Level Clouds:

In contrast with mid-level clouds, optically thin and medium low clouds show a negative *adjustment difference* between solp4p and 4xCO2 (**Figure 2**, orange color) with good model agreement in the midlatitude oceans (at least for optically thin clouds) and marine stratocumulus regimes including much of the Southern Ocean. Looking at the 4xCO2 adjustment (**Figure 3**, third row) there is a ubiquitous decrease in optically thin low cloud over subtropical and midlatitude ocean, and in the optically medium category there is cloud loss over most ocean regions. In combination, the mid- and low-level changes suggest that the tops of clouds residing in and near the boundary layer over subtropical and midlatitude ocean lower and that these clouds become optically thinner in response to increased CO_2. This marine cloud lowering and thinning is not present in the simulations with increased solar forcing, which show an increase in mid-level clouds over most ocean, and if anything, suggest a lifting and thickening of mid- and low-level clouds in some regions. Over most land on the other hand, there is decrease in low cloud in response to increased CO_2 in optically thin and medium cloud categories, at least in locations with good agreement between models (shown by stippling). The pattern of response to increases in solar forcing is similar to CO_2 over land, but with decreases in low- and mid-level cloud being stronger in the adjustment to CO_2, resulting in a positive *adjustment difference* over land. We will discuss the mechanisms responsible for the cloud adjustment described here in Section 4, but before doing so we turn our attention to the radiative impact of these adjustments.

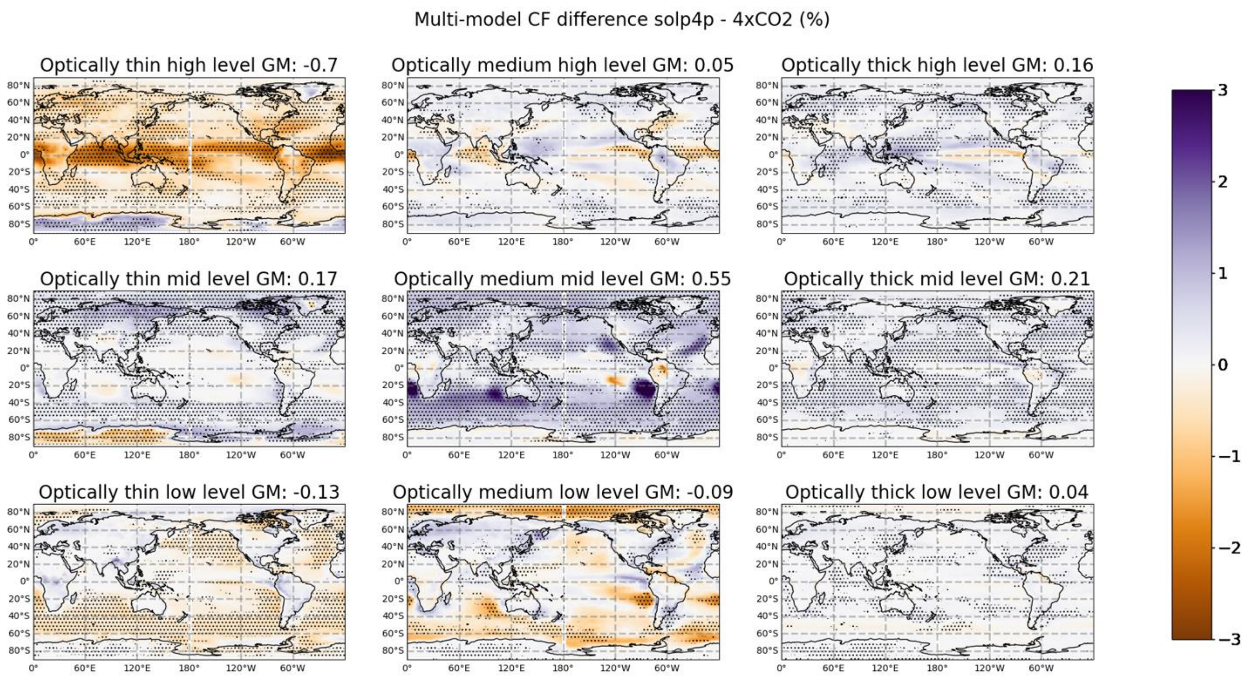

***Figure 2** Multi-model mean of the adjustment difference estimated following Equation 2. Stippling indicates regions where at least three out of four participating models agree on the sign of the adjustment difference.*

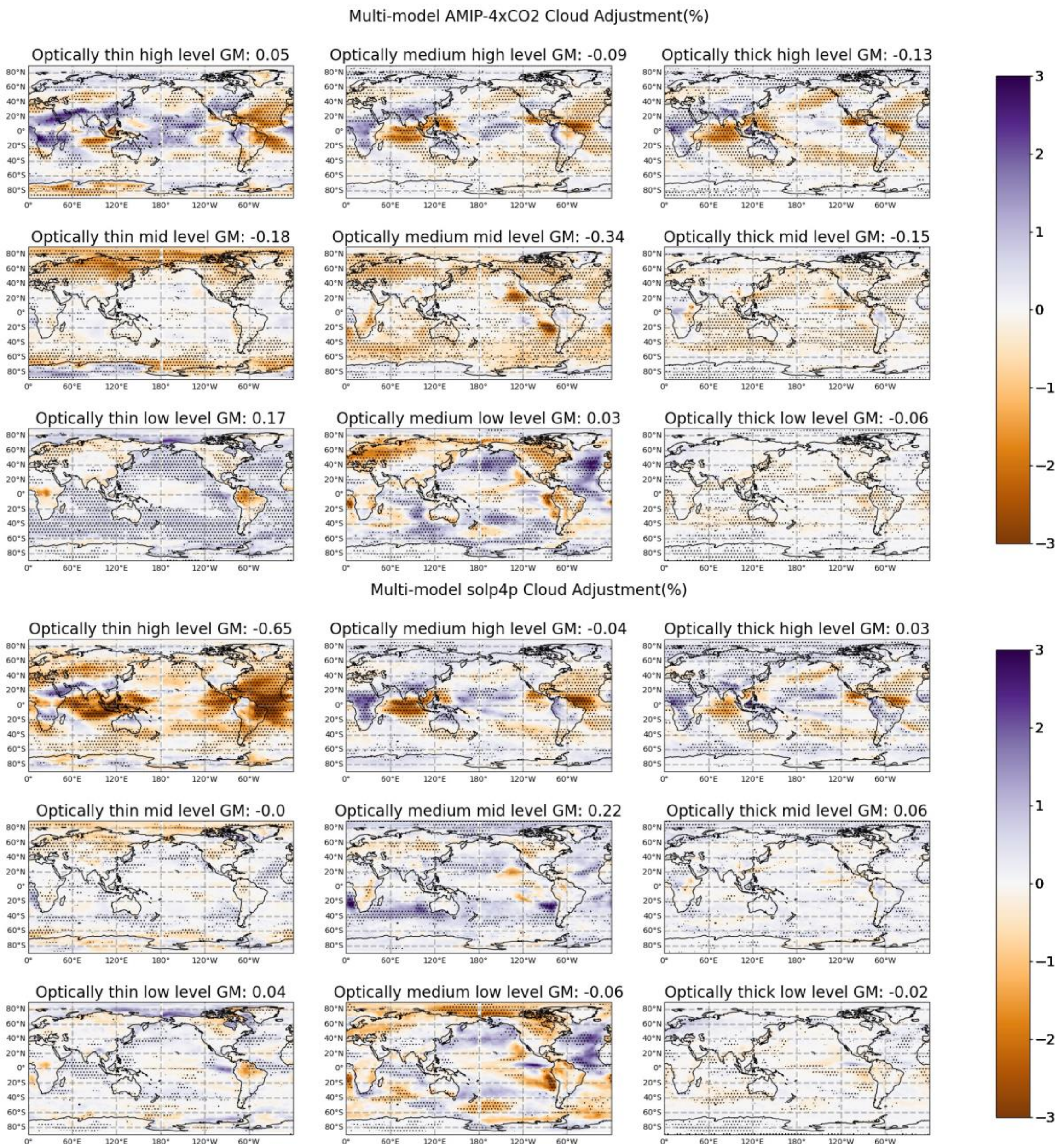

***Figure 3** Top 3 rows: multi-model mean adjustment of cloud amount in nine categories calculated from 30 year long averages of the amip-4xCO2 experiment, where the atmospheric CO_2 is quadrupled while the sea-surface temperature and sea-ice are held fixed. Bottom 3 rows: multi-model mean estimated adjustment of cloud amount in nine categories calculated following Equation 2.*

3.2 Top of Atmosphere Cloud Radiative Effect

The cloud adjustments previously described alter the Earth radiation budget, and thereby enhance or diminish the effective radiative forcing (depending on the change). The Cloud

Radiative Effect (CRE) can be calculated in many ways such as directly from top-of-atmosphere radiation output (e.g. Su et al., 2010), Partial Radiative Perturbation (Taylor et al., 2007), or cloud radiative kernels (Zelinka et al., 2012a). Here we use cloud radiative kernels because they are simple to use and provide a direct link with cloud changes described in Section 3.1. CRE from radiative kernels are calculated directly from changes in the underlying cloud distribution and are independent of cloud masking effects (changes in non-cloud variables that impact top-of-atmosphere radiation and how it is impacted by cloud) (Zelinka et al., 2013). On a minor note, we have multiplied the shortwave kernels by a factor of 1.04 in the solp4p calculations to account for the increased insolation. The effect of this adjustment is small and has no impact on the conclusions drawn from the application of cloud radiative kernels to these experiments as the differences noted between the CRE changes in the different experiments are greater than this 4% change.

In **Figure 4** we show the global mean CRE adjustment to 4xCO2 and solp4p (meaning the radiative effect of the cloud adjustment calculated from the fixed-SST experiment for 4xCO2, and following Equation 3 for solp4p) separated into the LW, SW, and NET radiative effect resulting from adjustments in CTP, optical depth, and Cloud Fraction following the Zelinka et al. (2012b) decomposition. In the Supplemental Materials we partition the radiative effect into the contributions from low, mid-level, and high-cloud adjustments. The NET adjustment is simply the sum of the LW and SW components.

In the shortwave component (top row of **Figure 4**) the CRE of both the solp4p *estimated adjustment* and AMIP-4xCO2 adjustment are positive across all models except for the adjustment of MRI-ESM2-0 to solp4p (in which there is a strong negative SW adjustment from mid-level clouds). In the multi-model mean (blue and orange bars) there is a greater positive SW radiative adjustment from 4xCO2 than solp4p. This is due to differences in the optical depth component of the SW radiative adjustment, where there is a positive adjustment to 4xCO2 that is consistent across models, and a negative SW adjustment in the solp4p. The difference is especially notable in the high cloud category (see **Supplemental Materials**). There is also considerable difference in the radiative effect of CF adjustments, where there is a more positive SW adjustment to solp4p than 4xCO2 for all models but MRI-ESM2-0 such that the multi-model mean SW adjustment is more positive to solp4p than 4xCO2. The difference in CF adjustment is quite pronounced in both the low and high-cloud categories. Not surprisingly, CTP changes have little effect on the SW, and there is very little SW radiative effect from CTP adjustments.

In the longwave component (middle row of **Figure 4**) the 4xCO2 total adjustment is negative across all models, meaning that the LW cloud adjustment has a cooling effect on the climate. In the multi-model mean the total LW adjustment to solp4p is also negative (albeit less so than the adjustment to 4xCO2), however in HadGEM3-GC31-LL there is a positive total adjustment (which is mostly due to the CTP adjustment of that model to solp4p being far more positive than the other models', signifying that it has a net decrease in CTP or rising cloud tops), and in MRI-ESM2-0 there is a small but positive total LW adjustment, because in this model the adjustment to solp4p includes a global mean increase of low and mid-level cloud fraction. All models aside from MRI-ESM2-0 produce a more negative LW CF adjustment to solp4p than 4xCO2 (which, similar to the SW component, is due to CF adjustments in the low and high-cloud categories). There is also a difference in the LW optical depth adjustment to solp4p and 4xCO2. There is near-zero LW optical depth adjustment to 4xCO2 in all models, and a positive LW optical depth adjustment to solp4p (which we show in the **Supplemental Materials** is mostly due to the high-cloud changes).

In the bottom row of **Figure 4** we show the shortwave and longwave components summed together as the NET radiative adjustment. The total NET adjustment is positive in all models for 4xCO2, and all but MRI-ESM2-0 for solp4p. In the multi-model mean the total NET adjustment to 4xCO2 is more positive than to solp4p. However, we note that the inter-model spread is greater in the adjustment to solp4p, such that in IPSL-CM6A-LR and CanESM5, the total NET adjustment to 4xCO2 is in fact smaller than to solp4p. We find that the largest difference in the total NET adjustment comes from the optical depth adjustment of high clouds, where there is thickening due to solp4p, and thinning due to 4xCO2.

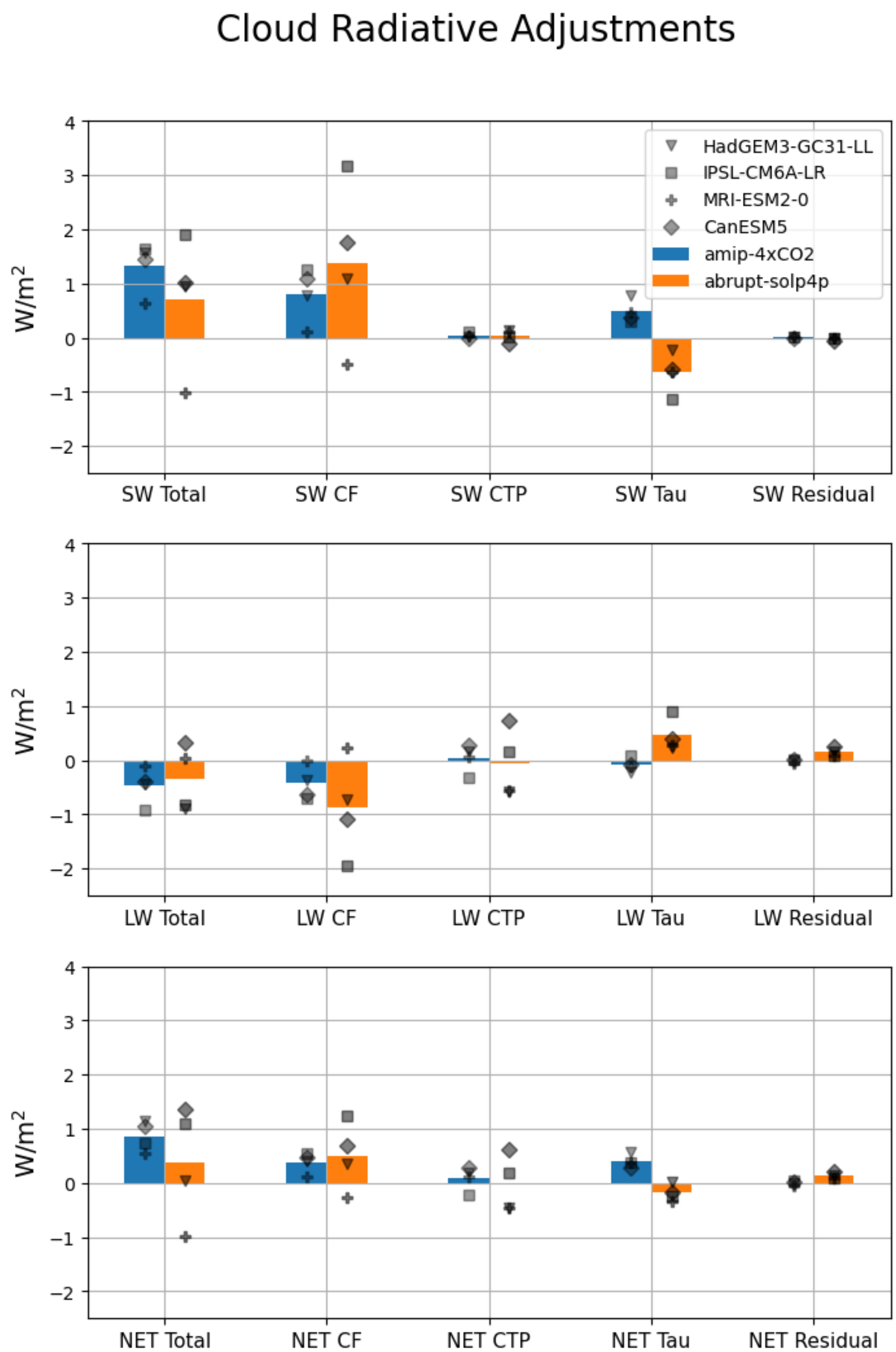

Figure 4 *Bar chart of the global mean radiative adjustment to 4xCO2 (blue) and solp4p (orange) for the shortwave (top row), longwave (middle row) and net (bottom row) component of the cloud radiative effect calculated with cloud radiative kernels. Bars indicate the multi-model mean; black symbols indicate individual model values.*

In **Figure 5** we show spatial maps of the SW, LW, and NET total adjustment to solp4p and 4xCO2 and the *adjustment difference* to highlight some locations where the adjustment of

CRE is noteworthy. In the **Supplemental Materials** we provide additional figures showing the radiative effect of CF, CTP, and optical depth adjustments broken down by low, mid-level, and high clouds. Beginning with the *estimated adjustment* to solp4p, there is positive adjustment over the Indian Ocean, the Tropical Atlantic, East Pacific, North America, most of Eurasia, the Southern Ocean, the Northern Pacific and Atlantic. Such is largely due to decrease in cloud fraction. In the **Supplemental Materials** we show that the positive cloud radiative adjustment to solp4p over the Indian, Atlantic, and East Pacific oceans is due to reduction in high cloud, we likewise find a negative LW adjustment in these regions (as is expected from high-cloud reduction). In contrast, the positive adjustment over Northern Hemisphere continents, and the North Atlantic and Pacific, and Southern Ocean are due to low-cloud reduction, in these locations there is little LW response, because low-clouds have similar emission temperature at cloud top as the surface, so they have little LW radiative effect. Thus, when combined, the NET adjustment to solp4p is positive, and is strongest in regions with low-cloud reduction (over Southern Ocean, and Northern Midaltitude ocean and continents), with a negative contribution in the Tropical Atlantic and East Pacific (from CTP reduction). We also point out that in the NET there is some positive radiative effect of the cloud adjustment to solp4p over the Peruvian and Californian Stratocumulus where there is reduction of low-level cloud.

In the 4xCO2 many of the patterns of adjustment are similar to the solp4p (as is expected from the similarity in cloud adjustments shown in **Figure 3**), for instance, there is a positive SW and negative LW radiative adjustment over the Indian Ocean and Tropical Atlantic due to high-cloud CF change such that they sum to nearly zero NET radiative effect. There is also a positive response SW in the Southern Ocean and Stratocumulus regimes due to change in low-cloud CF. There is however, a positive NET radiative adjustment in stratocumulus regimes which is greater and more widespread than the adjustment to solp4p, and in contrast to the solp4p (where the stratocumulus adjustment is mostly from low-clouds), in the 4xCO2, this is due mostly to a reduction of mid-level cloud.

There are a handful of other key differences in the radiative effect of adjustments to solp4p and 4xCO2, which are shown in the bottom row of **Figure 5**. For instance, in the North Pacific, the radiative effect of low-cloud adjustment to solp4p is greater than that of 4xCO2, such that the *adjustment difference* is positive in the SW and the NET. There is additionally, a large negative SW and positive LW adjustment difference in the Tropical Pacific, which we show in the **Supplemental Materials** is due to high-cloud optical depth adjustment. In the Tropical Atlantic and Indian Oceans, there is a positive SW and negative LW *adjustment difference*, due to the greater high-cloud CF reduction that occurs in solp4p than 4xCO2. There is also a significant *adjustment difference* in stratocumulus regimes, where there is negative SW and positive LW *adjustment difference* due to a combination of low and mid-level CF adjustments. Over land surfaces, the *adjustment difference* varies by location, and has sparse model agreement. One region however with good model agreement is Northern Europe, where there is a negative SW *adjustment difference*, and a weak LW *adjustment difference*, such that the NET is negative. In the **Supplemental Materials** we show that this change is mostly due to mid-level and low clouds. There is also good agreement on the *adjustment difference* over Northern Africa, where there is a weak positive SW *adjustment difference*, and a negative LW, such that the NET is negative due to changes in CF of high clouds (see **Supplemental Materials**).

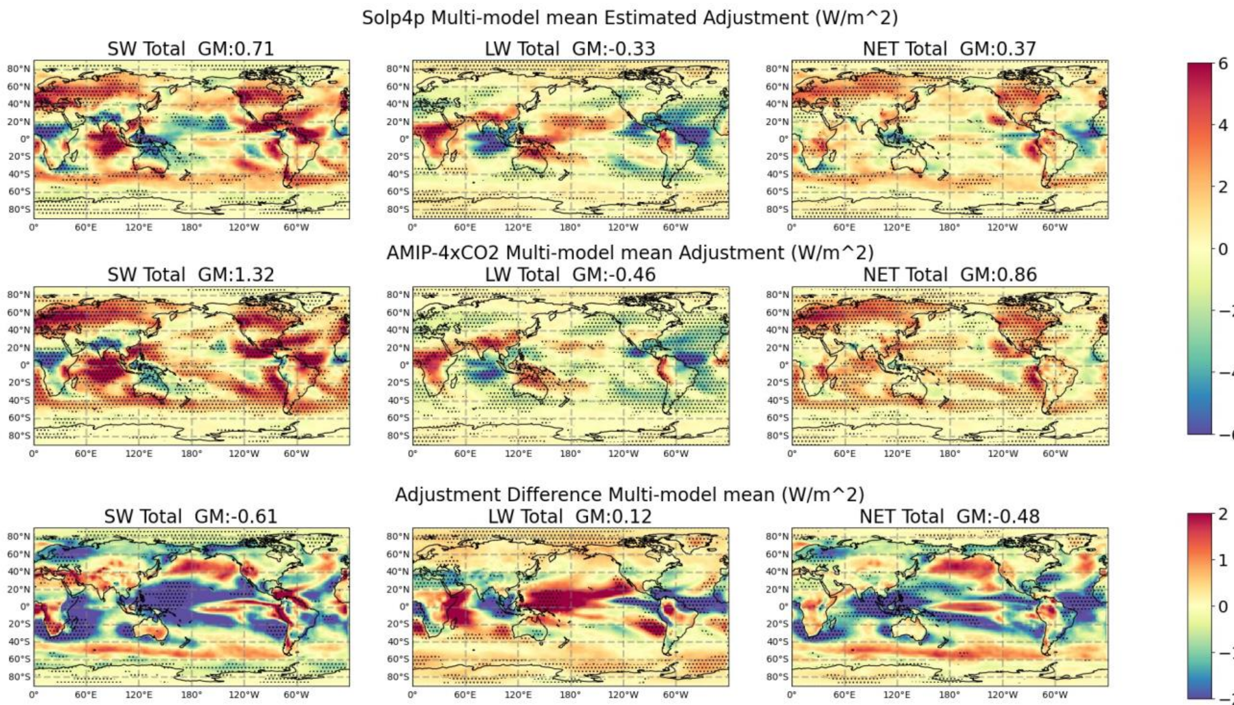

Figure 5 *Maps of SW, LW, and NET total adjustment to solp4p (top row), 4xCO2 (middle row), and the adjustment difference (bottom row). As with previous figures, stippling indicates regions where at least 3 out of 4 models agree on the sign of the response.*

3.3 Cloud Controlling Factors

In this subsection we apply the same formalism as before (Equation 3) to non-cloud variables that previous studies have shown influence clouds. Specifically, we calculated the *adjustment difference* as in Equation 4, where X is some non-cloud variable; and we calculate the solp4p *estimated adjustment* of X, as in Equation 5 by adding the adjustment calculated for 4xCO2 based on differencing averages of the AMIP and AMIP-4xCO2 experiments.

$$\Delta \mathrm{A}_{\mathrm{sol-CO2}}(\theta,\phi) = \langle \mathrm{X}_{\mathrm{sol}}(\theta,\phi,\mathrm{t})\rangle_{\mathrm{t}=10-150} - \langle \mathrm{X}_{\mathrm{CO2}}(\theta,\phi,\mathrm{t})\rangle_{\mathrm{t}=10-150} \quad (4)$$

$$A_{\mathrm{sol}}(\theta,\phi) = \Delta \mathrm{A}_{\mathrm{sol-CO2}}(\theta,\phi) + A_{\mathrm{CO2}}(\theta,\phi) \quad (5)$$

In **Figure 6** we show the adjustment to solp4p and 4xCO2 in the surface temperature and 500 hPa vertical velocity. Not surprisingly, the 4xCO2 surface temperature adjustment shows significant increases over land and sea ice, and near zero temperature change over ocean (which is equivalent to sea-surface temperature and will hereafter be referred to as such). This result is inherent to the experimental design where 4xCO2 adjustment is calculated from fixed-SST simulations in which the sea-ice surface temperatures are fixed. The surface temperature *adjustment difference*, on the other hand, is not constrained to be zero at any location, and the *adjustment difference* includes differences in temperature pattern (which are not mediated by global mean temperature); and consequently, our solp4p *estimated adjustment* likewise includes the effects of deviations in the surface temperature from the 4xCO2 pattern. In particular, the *adjustment difference* plot in the bottom left panel of **Figure 6** shows that in the solp4p there is more warming in the tropics and less warming in the poles as compared with 4xCO2. One can certainly interpret this change in surface temperatures as a limitation (or error) in our estimated solp4p adjustment technique, but in some respects, there is a philosophical question regarding what should or should not be considered an adjustment. We address this point further near the end of **Section 4**. Regardless, the point remains that increase in CO_2 and insolation result in slightly different patterns of surface warming.

The 500 hPa vertical velocity indicates changes in large scale circulation, where positive anomalies (green) indicate regions with diminished convection or enhanced subsidence. The pattern of changes in the *estimated adjustment* to solp4p and 4xCO2 are similar, with 1) strong upward anomalies (purple colors) over most land equatorward of 40° latitude, 2) downward anomalies (green colors) over most tropical and subtropical oceanic regions of ascent (dashed contours) including the Tropical Atlantic and Indian Oceans, indicative of diminished convection and 3) upward anomalies over most tropical and subtropical oceanic regions of descent (solid contours) including the subtropical Pacific (20° to 40° latitude), and the subtropical Indian Ocean (-20° to -40° latitude), indicative of diminished subsidence. There is mixture of upward and downward anomalies over the midlatitude oceans (latitudes poleward of 40°) depending on the location; with perhaps the strongest and most significant feature being downward anomalies over much of the eastern North Pacific and North Atlantic.

Figure 7 shows the adjustment of Estimated Inversion Strength (hereafter referred to as EIS), and relative humidity at 700 hPa. The EIS is well correlated with the global low cloud occurrence in observations and models (Qu et al., 2014; Wood & Bretherton, 2006). The left column and top row of **Figure 7** shows that *adjustment differences* in the EIS of solp4p and 4xCO2 adjustments are generally small or modest except at high latitudes and land areas in the Northern Hemisphere. Over most ocean areas, the individual adjustments show increasing inversion strength, with greater inversion strengthening occurring in the solp4p than 4xCO2 in the North American and South American Stratocumulus regions. This result is expected because EIS depends on the difference in potential temperature between the surface and 700 hPa, and thus heating the troposphere (whether by solar forcing or CO_2 increase) while fixing SST (in the 4xCO2 adjustment or global mean temperature in the solp4p adjustment) will inherently increase the inversion strength. Over land and sea ice, the surface temperature is not fixed in the fixed-SST simulations and the negative EIS adjustment simulated here are likely artifacts of (or at least strongly affected by) the methods used to calculate the adjustments.

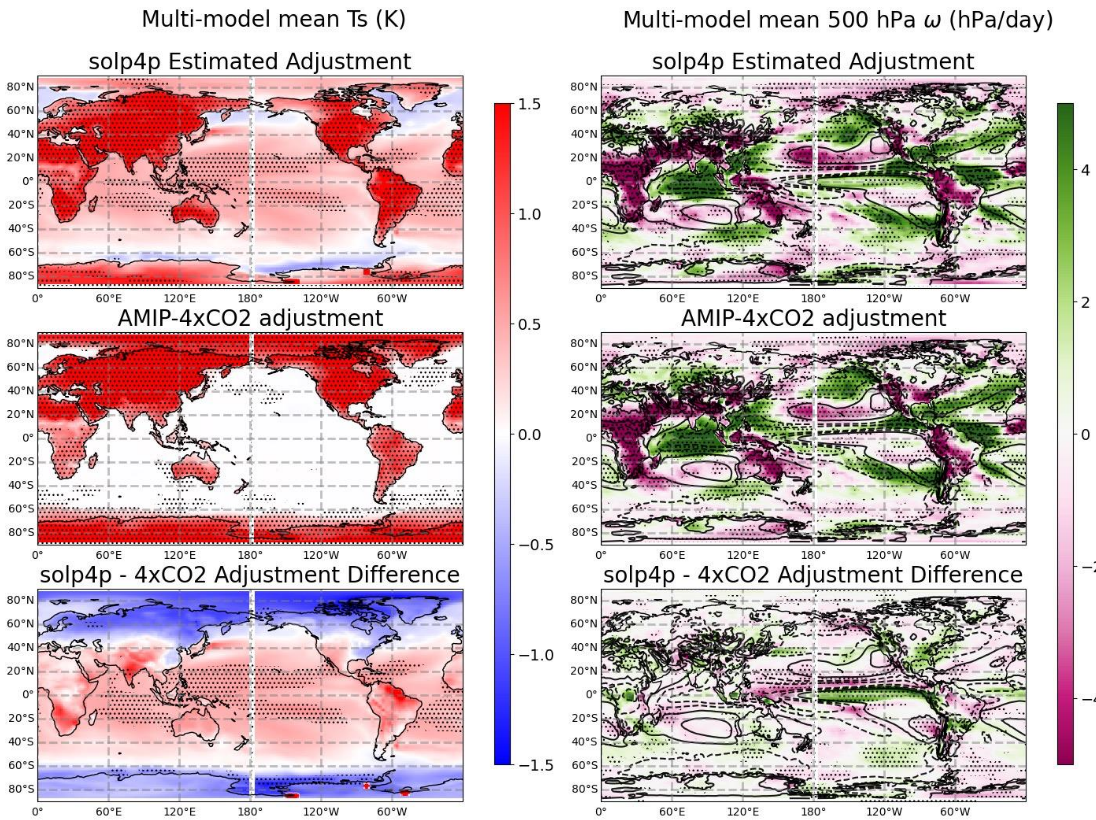

Figure 6 *Top row: Adjustment to solp4p of surface temperature (Ts) and 500 hPa vertical velocity. Middle row: Adjustment to Ts and 500 hPa vertical velocity calculated using the AMIP-4xCO2 experiment. Bottom row: the adjustment difference between solp4p and 4xCO2 for Ts and 500 hPa vertical velocity. As previously, stippling indicates regions where at least 3 of 4 models agree on the sign of the response. In the right column, the contours represent the piControl climatology, where dashed contours are regions with mean-state upward motion and solid contours are mean-state downward motion.*

Turning attention to the relative humidity at 700 hPa (hereafter RH_700), the right panels of **Figure 7** indicate the moisture availability of the free troposphere. The moisture difference between the surface and the free troposphere has a large impact on the efficiency of turbulent entrainment-driven drying of the boundary layer and has a large effect on the occurrence of low and mid-level clouds. The right panels of **Figure 7** show that in both the adjustment to solp4p and 4xCO2 there is a reduction of RH_700 in the midlatitude and polar regions (poleward of 30° latitude). There is also an increase of RH_700 over Central Africa, the Eastern Equatorial Pacific, and parts of the subtropical Pacific (especially in the northern hemisphere). While the patterns are similar, there is a positive *adjustment difference* (bottom panel) in nearly all regions further than 20° from the equator, meaning that the free troposphere is less dry in solp4p than 4xCO2; while the opposite is true in the adjustments in the equatorial Pacific and Atlantic.

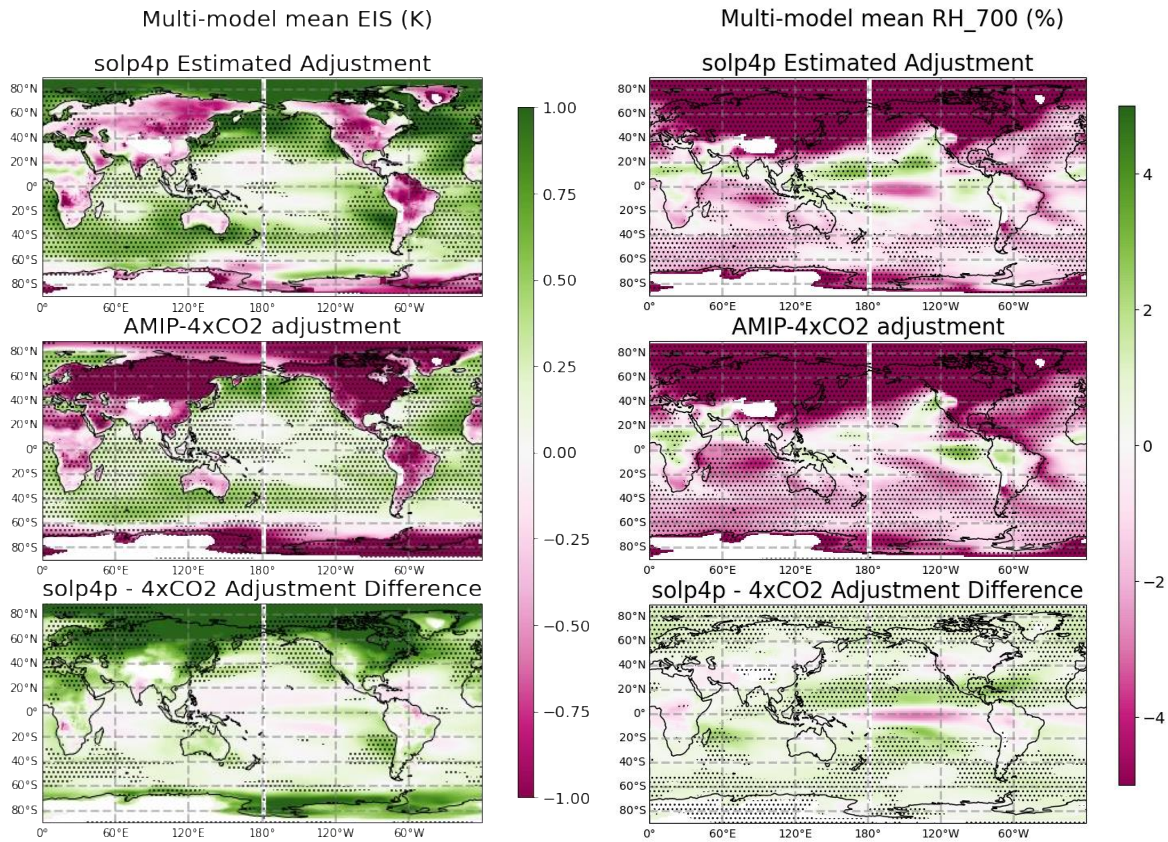

Figure 7 *Top row: Adjustment to solp4p of Estimated Inversion Strength (EIS) and 700 hPa relative humidity (RH_700). Middle row: Adjustment to Ts and RH_700 calculated using the AMIP-4xCO2 experiment. Bottom row: the adjustment difference between solp4p and 4xCO2 for Ts and RH_700. As previously, stippling indicates regions where at least 3 of 4 models agree on the sign of the response.*

3.4 Tropical Temperature Profile

The large difference in the adjustment of optically thin high-level cloud between the solp4p and 4xCO2 simulations draws attention to potential differences in the temperature profiles in the tropical pacific. **Figure 8** shows vertical profiles of temperature and equivalent potential temperature in the Indian Ocean and Tropical West Pacific (60 to 180° longitude and -15 to 15° latitude) for the solp4p and 4xCO2 experiments, as well as the *adjustment difference* between the equivalent potential temperature from the two experiments. We have isolated the Indian Ocean and West Pacific because it is a large region of mean-state ascent, and in **Figure 2** we show that there is a large difference in the occurrence of optically thin high cloud between the solp4p and 4xCO2 in the Indian and Western Pacific Oceans. Additionally, gravity waves caused by deep convection homogenize the temperatures aloft such that the temperature aloft throughout the tropics is set by the temperature profile in regions of ascent (Bretherton & Smolarkiewicz, 1989; Mapes, 1993; Sobel & Bretherton, 2000). In regions of ascent, the temperature profile is typically near that of a moist adiabat rising from the surface, such that temperature variations at the surface tend to be amplified aloft. As can be seen in the right-hand panel of **Figure 8** the upper atmosphere is warmer in the solp4p than the 4xCO2 in the multi-model mean, and the difference is larger in the upper atmosphere than at the surface. In IPSL-CM6A-LR the surface is in fact cooler in the solp4p than 4xCO2 (albeit only slightly), but the upper-atmosphere is warmer.

There are two aspects of the solar and CO_2 forcing mechanisms that likely contribute to the differences in the tropical temperature profile. 1) As previously noted, solar forcing is most effective at low latitudes, where insolation is strongest, so even when the global mean surface temperature change is the same, solar forcing causes greater tropical temperature increase than CO_2 (Kaur et al., 2023), and 2) CO_2 forcing preferentially heats the lower troposphere, while solar forcing induces anomalous heating which is homogenous through the troposphere (Salvi et al., 2021), hence solar forcing warms the upper atmosphere more efficiently than CO_2 forcing.

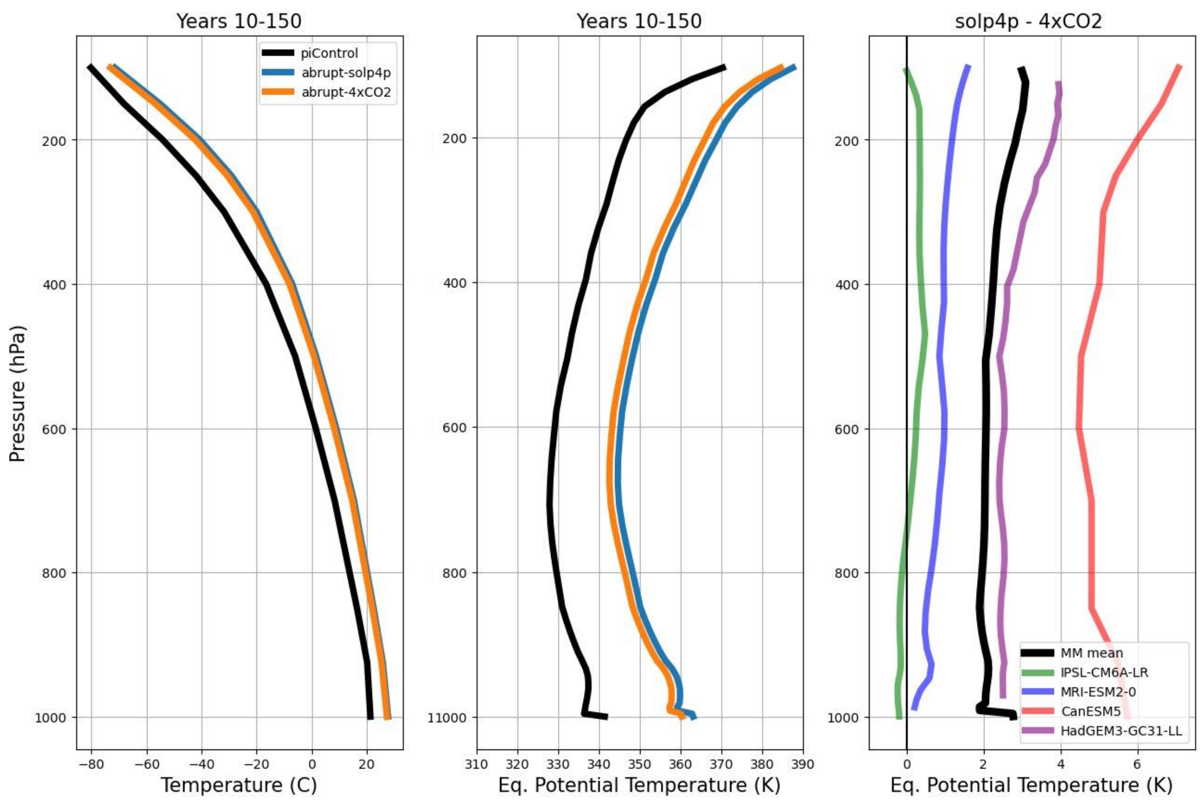

Figure 8 *Temperature and Equivalent Potential Temperature vertical profile in the Indian Ocean and tropical west pacific. Which is defined as ocean area between -15° to 15° latitude and 60° to 180° longitude. It is shown as the vertical profile of the multi-model mean from years 10-150 and the difference between the solp4p and 4xCO2 averages.*

4. <u>Discussion</u>

In this section we discuss the cloud adjustment to solp4p and 4xCO2 in the context of previous literature and the adjustment of cloud controlling factors shown in Sections 3.3 and 3.4. In Sections 4.1 and 4.2 we focus on high clouds and low and mid-level clouds respectively and hypothesize on the mechanisms contributing to the cloud adjustments. Then in Section 4.3 we discuss our findings in the context of previous studies on cloud adjustment to solar and CO_2 forcing. Finally, in Section 4.4 we discuss the possible limitations of the methods used in our study, and the ways that future work on this topic could reduce the uncertainty in their estimations of adjustment.

4.1 <u>High Clouds</u>

In the high cloud adjustments to both 4xCO2 and solp4p there is a decrease in high cloud fraction at all optical depths in the Tropical West Pacific, Tropical Atlantic, midlatitude oceans (between 20° to 60° latitude), and the eastern portion of Amazonia. There is increase in high cloud over the central Pacific (especially for medium and high optical thickness), and over tropical land masses such as Africa and Southeast Asia. The patterns of change are quite similar between the adjustment to 4xCO2 and solp4p (for at least optically medium and optically thick high cloud), and as one might expect, there is a strong correspondence of these changes with adjustments in the 500 hPa vertical velocity described in Section 3.3 (**Figure 6**). In short, there is a decrease in high cloud fraction where there are positive anomalies in the 500 hPa vertical pressure velocity (either increased downward motion or decreased upward motion) indicative of regions with diminished convection or enhanced subsidence and vice versa for negative anomalies.

Despite the similarity in the overall pattern, there are distinct differences between the cloud adjustments to solp4p and 4xCO2, and we focus the remaining discussion in this section on these differences. Specifically, we focus on the *adjustment difference* of optically thin, and optically medium and thick high clouds respectively.

Optically thin: There are fewer optically thin high clouds in the solp4p than in the 4xCO2 experiment. Many optically thin high clouds form via horizontal detrainment from deep cumulonimbus convective clouds, where moisture detrains horizontally in anvils that either directly form thin cirrus clouds or deliver moisture to the upper atmosphere that can form clouds in response to lifting by a variety of dynamical mechanisms including gravity and kelvin waves (Immler et al., 2008; Spichtinger et al., 2005). Cirrus clouds can exist in the upper-troposphere for a long time because the cold temperatures maintain slow sublimations rates of cloud particles (Seeley et al., 2019), and a circulation induced by differential radiative heating at cloud base and cloud top advects water vapor into the cloud, maintaining ice-crystal growth even in the presence of radiative heating (Dinh et al., 2010). Seeley et al. (2019) use cloud resolving simulations to show that, to first order, cloud lifetime in the upper troposphere is determined by the lifetime of condensate, and thus, the upper-tropospheric temperature. Solar forcing can be expected to heat the upper troposphere more than CO_2 (Salvi et al., 2021), and indeed we find the upper troposphere is warmer in the solp4p experiment than in the 4xCO2 experiment (**Figure 8**). We hypothesize this diminishes the saturation deficit through the Clausius-Clapeyron relationship and leads to a higher sublimation rate of high-cloud particles, and consequently shorter-lived anvil clouds and less thin cloud in solp4p than in the 4xCO2 experiment. Increased LW heating at cloud base in the 4xCO2 experiment could increase turbulent mixing and in principle might also prolong high cloud lifetime in this experiment (consistent with a smaller loss of high thin cloud), but such turbulent mixing occurs on spatial scales that are not resolved by climate models, and so is not a factor in the present results.

Optically medium and thick high clouds: We find more optically medium and thick high clouds occur in solp4p than 4xCO2, especially in regions of ascent such as the Tropical West Pacific, ITCZ and SPCZ (positive *adjustment difference* in **Figure 2**). This difference is largely due to a smaller loss of optically medium and thick clouds in the solp4p experiment compared with the 4xCO2 experiment in the Atlantic and Tropical West Pacific, however in the ITCZ and SPCZ, the change in optically medium and thick high clouds has poor agreement among models in the adjustment to solp4p and 4xCO2, yet there is good agreement on the *adjustment difference* of high medium and thick clouds in these regions.

We show in **Figure 8** that there is a positive *adjustment difference* of sea-surface temperature in the Tropical West Pacific, ITCZ and SPCZ. Higher sea-surface temperature potentially provides more latent and sensible heat release into the lower atmosphere of solp4p, destabilizing the atmosphere. Certainly, the *adjustment difference* in mean 500 hPa vertical velocity (**Figure 6** bottom panels), shows a smaller reduction in vertical velocities in the Tropical West Pacific, ITCZ and SPCZ ascent regions, and much of the mid-latitudes in the solp4p than in the 4xCO2 experiment. This suggests that the difference in optically medium and thick high cloud is linked to differences in the strength of the circulation response – a dynamical difference likely resulting from differences in the pattern of surface heating (rather than a direct radiative response).

4.2 Low and Mid-Level Clouds

Perhaps the most striking difference between the solp4p and 4xCO2 adjustments is the large and widespread decrease in mid-level clouds in the 4xCO2 adjustment as compared to the increase in mid-level clouds in the solp4p adjustment. This is perhaps most clear in the plot of the *adjustment difference*. **Figure 2** shows that this difference in mid-level cloud response is widespread and occurs over both land and ocean. The mid-level *adjustment difference* is largest for optically medium clouds and is especially large over regions occupied by marine stratocumulus clouds; and there is a corresponding *adjustment difference* of low-level clouds (at least for optically medium and thin low-level clouds) that is of the opposite sign over land and most oceanic areas. We will return to clouds over land momentarily, and first focus on marine cloud.

Although marine stratocumulus and cumulus clouds are often thought of as low clouds, the tops of these clouds sometimes reach altitudes where the pressure is measured below (at a higher altitude than) 680 hPa in both models and observations (Tselioudis et al., 2021; Zelinka et al 2022). As such, dynamic and thermodynamic changes to stratocumulus and cumulus clouds can have apparent impacts on both the low and mid-level cloud category. Taken as a whole, we interpret the combination of ISCCP low and mid-level cloud changes to mean that there is a net increase in the cloud-top-height (CTH) in boundary layer marine clouds in the solp4p adjustment and the opposite (a reduction of CTH) in most marine clouds in the 4xCO2 adjustment.

In trying to understand these low and mid-level cloud changes we follow the framework of Bretherton (2015), who attribute changes in boundary layer clouds (especially stratocumulus) to four primary mechanisms: 1) The *radiative effect* of water vapor and CO_2 in the free troposphere, where increases in water vapor or CO_2 warms cloud-tops and results in a lowering of cloud-top and a thinning or reduction in cloud amount. 2) *The dynamic effect* related to changes in subsidence where a decrease in subsidence results in rising cloud-tops and a thickening or increase in cloud amount. 3) *the thermodynamic effect* related to changes in surface temperature and free tropospheric relative humidity where an increase in surface temperature or decrease in free tropospheric relative humidity results in thinning or decrease in cloud amount. And finally 4*) the stability* effect related to changes in inversion strength where strengthening inversions result in a lowering of cloud-top and thickening or increase in cloud amount. In the following paragraphs we first discuss the cloud adjustments to solp4p and 4xCO2 individually, before turning attention to the *adjustment differences*.

Marine Clouds Solp4p: In the low and mid-level cloud adjustment to solp4p (**Figure 3**) there is a lifting of cloud top and a net increase in the low and mid-level cloud amount in stratocumulus regimes. We find in **Figure 6** that there is also subsidence decrease in stratocumulus regimes (upward vertical velocity adjustments in regions with climatological subsidence). The *dynamic effect* predicts an increase in cloud-top-height and cloud amount with decreasing subsidence. Hence, we find that the reduction in low cloud and increase in mid-level cloud adjustment in stratocumulus regions is consistent with decreases in subsidence rate to solp4p. This effect appears to play a critical role in the total cloud response, as none of the other Bretherton (2015) effects explain the increase in CTH. There is a reduction in 700 hPa relative humidity (top right panel of **Figure 7**) which is expected to thin or reduce cloud amount via *the thermodynamic effect*, though in general, the reduction in relative humidity is not strong in stratocumulus regions. The increase in solar flux will only slightly warm cloud-tops such that *the radiative effect* of solp4p is likely to be small and would also be expected to cause cloud thinning or decrease in cloud amount and a lowering of cloud tops. There is a strong increase in EIS in stratocumulus and trade-wind regions, which is consistent with the net increase in low and mid-level cloud fraction in these regions, however *the stability effect* also predicts a decrease in CTH, which is again opposite what we find in the stratocumulus regions in the solp4p experiment. Of course, one expects that all the effects described by Bretherton (2015) occur to varying degrees; nonetheless it appears that *the dynamic effect* is having a large impact in the subtropical stratocumulus dominated regions in the cloud adjustment to solp4p.

In parts of the midlatitudes such as the Southern Indian Ocean, the North Pacific, and the North Atlantic, there are increases in both low- and mid-level cloud amount (**Figure 3**). For example, in the North Pacific, the low cloud adjustment (averaged from 150° to 220° longitude, and 40° to 60° latitude) is 0.89% and the mid-level cloud adjustment is 0.30%, so the increase in low clouds is greater than mid-level clouds in these locations. In combination with the large positive adjustment in EIS, this suggests that *the stability effect* is playing a stronger role in the solp4p cloud adjustment at these higher latitudes, though a smaller (offsetting) contribution from *the thermodynamic effect* (as there is more surface warming in the adjustment at lower latitudes) is also likely a factor in the different response in solp4p between mid-latitudes and the subtropics.

Marine Clouds 4xCO2: In the adjustment to 4xCO2 there is widespread decrease in mid-level cloud and increase in low-level cloud in most oceanic regions such that when the low- and mid-level cloud is combined there is net decrease in CTH and reduction in cloud amount. These cloud changes occur over effectively all ocean surfaces but are greatest over stratocumulus regimes. Of the four mechanisms from Bretherton (2015), only *the radiative effect* predicts that with increasing CO_2 there will be a lowering and thinning or reduction of boundary layer clouds consistent with the cloud adjustment in stratocumulus regions. And *the radiative effect* from CO_2 increase has been studied using high-resolution large-eddy simulating models to show that there is in fact a certain CO_2 threshold (for a fixed subsidence rate) that when surpassed causes stratocumulus decks to dissipate into open-cumuli (Schneider et al., 2019), resulting in decreased cloud fraction and cloud-top-height. There is widespread decrease in relative humidity at 700 hPa, and no change in sea-surface temperature (by experimental design). *The thermodynamic effect* predicts thinning or decrease of cloud with free-tropospheric drying (when there is no sea-surface temperature change). There is also increase in EIS over midlatitude oceans and marine-stratocumulus regions, and *the stability effect* leads to thickening or increase in cloud amount and CTH reduction with increasing EIS. We in fact, do find that the adjustment to 4xCO2 includes a decrease in CTH of stratocumulus and cumulus clouds, and in the trade-wind regions there is increase of medium and thin clouds (when summed together). Also, like the solp4p, the adjustment to 4xCO2 includes weakening of subsidence (upward anomalies in regions of mean-state subsidence in **Figure 6**) over the Californian and Australian stratocumulus regimes, so in these locations *the dynamic effect* is counter-acting the radiative effect and is likely damping the thinning and decreasing CTH of stratocumulus cloud shown in **Figure 3**. As in the solp4p, one expects that each of the four mechanisms contribute to the total cloud changes in different locations simultaneously. We find that the cloud adjustment to 4xCO2 in stratocumulus regions is quite consistent with that expected from *the radiative effect* due to the decrease in medium optical depth mid-level cloud and (lesser) increase in optically thin low-level cloud. However, we expect that there are counter-acting effects from *the stability and dynamic effects*, and some contribution to the cloud thinning and decrease from *the thermodynamic effect*. In the trade-wind regions the cloud changes are most consistent with *the stability effect* due to the decrease in CTH and increase in cloud amount, which is likely damped by *the thermodynamic effect*.

In both the adjustment to solp4p and 4xCO2, there is widespread increase in EIS. This is an expected result, because (as was previously mentioned) EIS depends on the difference in potential temperature between the surface and 700 hPa, so when SST is fixed, any atmospheric heating will inherently increase the inversion strength. Kamae et al. (2019) used model experiments where SST and land warming were held fixed to isolate the atmospheric adjustments from the effects of land warming. They find that atmospheric adjustments to 4xCO2 (without land warming) cause increased summertime EIS over midlatitude oceans and increased wintertime EIS in stratocumulus regions. They additionally find that land warming increases summertime EIS over midlatitude ocean but has little impact on EIS in stratocumulus regions. Hence, we expect that the EIS increase we see in both solp4p and 4xCO2 are due to a combination of land warming, and the adjustment of the atmosphere with fixed-SST.

Marine Clouds Adjustment Difference: As described at the beginning of this section, there is striking and widespread *adjustment difference* between solp4p and 4xCO2 experiments, with more mid-level cloud in most marine areas (including the stratocumulus regimes, mid-latitude and polar oceans) in the solp4p experiment relative to the 4xCO2 experiment, and a corresponding *adjustment difference* of low-level clouds (at least optically medium and thin low-level clouds) of the opposite sign. We expect that *the radiative effect* of CO_2 is likely the primary contributor to the *adjustment difference* in low and mid-level cloud for two reasons. First, unlike CO_2, solar forcing has little impact on cloud top radiative cooling. While there is likely some cloud adjustment to solp4p originating from the diabatic solar heating of clouds, this will be small compared to the effect of quadrupling CO_2, which will significantly reduce cloud top longwave radiative cooling. So, in short, one expects *the radiative effect* of $4xCO_2$ to be much larger. Second, the changes in the other cloud controlling factors do not match the broad pattern of *adjustment difference.* Specifically, the patterns of 500 hPa vertical velocity and EIS adjustments are broadly similar between the two forcing experiments. So, while there are small *adjustment differences* in the 500 hPa vertical velocity and EIS that almost certainly contribute somewhat to the cloud *adjustment difference* in some regions, the associated *dynamic and stability effects* seem unlikely to explain the broad pattern of the *adjustment difference*. Similarly, changes in SST, which are possible in the *adjustment difference* because of the approach we use (and which one might consider an error or limitation of the approach – see Section 4.4 for discussion of this point), are small in the midlatitudes and do not match the pattern of the cloud *adjustment differences*.

Land: To this point our discussion has focused on mid and low-level marine clouds for which the Bretherton (2015) framework is applicable. We now shift our focus to the cloud adjustments over land surfaces. Land warming in fixed-SST experiments certainly has a large influence on cloud adjustments over land via thermally induced circulations caused by the land-sea temperature gradient (Andrews et al., 2021a). We view this as a limitation of the fixed-SST approach, and as such, focus our discussion of land adjustments on *the adjustment difference* which does not rely on fixed-SST methods. In contrast to the marine cloud changes, over most land areas there are positive difference in cloud amounts (meaning more low cloud occurring following solp4p than 4xCO2 – see purple colors in **Figure 2**) in all optical depth and CTP categories, except for optically thin high cloud. The larger reduction in optically thin high clouds occurs over both land and ocean and appears (we speculate) to be a response that is not specific to land (see Section 4.1). In general, the high and mid-level cloud adjustments are broadly similar over land and ocean. This contrasts with the case of optically thin and medium low-level clouds, where there is persistently more low cloud over land in the solp4p than 4xCO2 experiment and the opposite (fewer low clouds) over ocean. Admittedly, there is poor model agreement on low cloud changes over land, but the delineation between land and ocean is distinct.

Over land, one of the primary sources of moisture is the latent heat fluxed from the biosphere into the atmosphere via evapotranspiration. In plant physiology there is a well-established effect of CO_2 increase where plant stomata do not open as wide, reducing the transfer of moisture and energy to the atmosphere through evapotranspiration, which we hereafter refer to as *the plant physiological effect* (e.g. Betts et al., 1997; Cox et al., 1999; Field et al., 1995). There is also the effect of solar forcing on evapotranspiration; increase in the amount of total SW radiation reaching the surface causes photosynthesis (and evapotranspiration) rates to increase (Mercado et al., 2009). In **Table 1** we show the *adjustment difference* in the global mean latent heat release from land surface. There is greater latent heat release in the solar forcing experiments than the 4xCO2, which we speculate contributes to the lesser amount of low and mid-level cloud simulated over most land areas in solp4p compared with 4xCO2 via *the plant physiological effect*. Chadwick et al. (2019) performed model simulations which separate the influences of 4xCO2 on land precipitation into the component that is due to land warming (in a fixed-SST experiment) and the *plant physiological effect.* They find that the *plant physiological effect* decreases precipitation over most land areas because of its impact on moisture availability. Along the equator in portions of Africa and South America (in the only two locations coincident with a negative *adjustment difference* of low-level cloud) they find an increase in precipitation, because of how the *plant physiological effect* impacts local surface temperature and causes surface convergence. Thus, we speculate that the cloud *adjustment difference* shown in **Figure 2** is likely a combined effect of CO_2 and solar forcing having opposite effects on evapotranspiration rates (and thus moisture availability) over most land areas, and the impact the *plant physiological effect* to CO_2 can have on dynamics in the tropics (specifically causing surface convergence).

Model	Land-Air Upward Latent Heat Flux Adjustment Difference (Wm^{-2})
IPSL-CM6A-LR	5.1
MRI-ESM2-0	1.0
CanESM5	2.8
HadGEM3-GC31-LL	5.1
MM mean	3.5

***Table 1** Adjustment difference of latent heat release from land surface to the atmosphere.*

4.3 Comparison With Previous Literature

As mentioned in the introduction, there are a handful of recent studies which have posed relevant questions to this study.

Firstly, in the GeoMIP G1 experiment CO_2 is abruptly quadrupled, and solar forcing is reduced such that the net global radiative forcing is zero, thus there is no global mean temperature change, so the total cloud response is equivalent to an adjustment to simultaneous solar and CO_2 forcing. Russotto & Ackerman (2018) examined the cloud changes in these experiments and found a reduction of stratocumulus clouds associated with a decrease in inversion strength, and an increase of high clouds along the ITCZ and SPCZ, and in the Indian Ocean. We similarly find a reduction of stratocumulus clouds from 4xCO2 that is not matched by the solp4p. However, we conclude that the role of EIS is in fact secondary in this *adjustment difference* and the direct radiative effect of solar and CO_2 forcing (where CO_2 more efficiently warms cloud tops and reduces LW cooling) is the primary driver. Concerning high clouds, we find that there is a negative *adjustment difference* between solp4p and 4xCO2 of optically thin high cloud, and positive *adjustment difference* of optically medium and thick high cloud, such that when combined, there is a negative *adjustment difference* of all high clouds that is largest in the Indian Ocean, ITCZ and SPCZ (see Supplemental Materials for combined figure). Thus, the cloud adjustments we find are consistent with the findings of Russotto & Ackerman (2018) for high clouds.

There is also the work of Salvi et al. (2021), which examines the adjustment to vertically localized heating experiments, to understand how the vertical heating profile of various forcing mechanisms (including solar and CO_2 forcing) impact cloud adjustment. They find that solar forcing (which is more top-heavy than CO_2) increases the amount of low cloud by increasing the strength of the boundary layer inversion. The effect is evident in the experiment analyzed here. Indeed, the solar forcing is more effective in warming the free troposphere, capping the moisture in the boundary layer. This effect is shown as the strengthening inversions in the solp4p experiment (**Figure 8**).

Through their study of the adjustment to a range of forcing agents simulated in PDRMIP Smith et al. (2018) found that cloud adjustments to CO_2 increase contributes a global mean positive net radiative forcing, while the cloud adjustment to solar forcing contributes a global mean negative net radiative forcing. Using the cloud radiative kernels, however, we find that there is a global mean net cloud radiative adjustment that is positive (0.37 W/m^2 and 0.86 W/m^2 respectively) for both solp4p and 4xCO2. Our finding that both forcing mechanism cause positive cloud radiative adjustments contrasts the Smith et al. (2018) result of opposite sign adjustments. It is unclear if the discrepancy between our results and those of Smith et al. (2018) are due to the different set of models used in each study, differences in the response to 2xCO2 and 2% solar forcing versus 4xCO2 and 4% increase in solar forcing, or if it is related to the method we use to calculate the *estimated adjustment* of solp4p. Regardless, this discrepancy highlights the importance of further constraining cloud adjustments (and not focusing only on the temperature mediated feedbacks), documenting cloud adjustments, and understanding of the underlying physical mechanisms. The latter of which, is especially important if we are to relate the results of process and regional models to the total cloud response. And more generally, it seems likely that differences between models are (to some extent) likely due to bias in the models' initial state. For example, two models with roughly the same response of stratocumulus to the radiative impact of CO_2 will have very different global mean response if one model has twice the stratocumulus as the other.

Regarding the differences in cloud adjustments to solar and CO_2 forcing over land, Modak et al. (2016) find that that *the plant physiological effect* of CO_2 causes there to be more clouds in the adjustment to solar forcing than CO_2. We indeed, find a similar result in the *adjustment difference* over land, where there is a positive *adjustment difference* in low-cloud.

4.4 Limitations of Estimated Adjustment Method

In this paper we have relied on forced fixed-SST simulations to calculate the adjustments to the forcing in the 4xCO2 experiment and subsequently to estimate the adjustments for the solp4p experiment. This fixed-SST method has been widely used in previous studies (e.g. Colman & McAvaney, 2011; Gregory & Webb, 2008; Smith et al., 2018; Zelinka et al., 2013), but is limited in that, while the sea surface temperature and the location of sea ice are fixed, the land surface is allowed to warm. A warming land surface does of course cause changes in atmospheric circulations to occur, and the global mean surface temperature is not constrained to be zero. Andrews et al. (2021a) compared AMIP-4xCO2 experiments with 4xCO2 experiments where both land and sea-surface temperatures were fixed. Many of the cloud adjustments in **Figure 3** are consistent with the adjustment that Andrews et al. (2021a) found are due to land warming. This includes a decrease in high cloud amount over the Atlantic and Indian Oceans, an increase in high cloud over land masses along the equator (especially over Central Africa), an increase in low cloud over midlatitude oceans (North Atlantic, North Pacific, and Southern Indian and Pacific Oceans), and a decrease in low-level cloud over continents especially in the optically medium low cloud category.

Our calculated *adjustment difference* does not rely on fixed-SST simulations; however, the *adjustment difference* is impacted by differences in warming pattern between solp4p and 4xCO2. More broadly, we stress that our *estimated adjustment* does not work for all model experiments, and in fact is only effective because 1) in solp4p there is a similar amount of warming as 4xCO2, and 2) the temperature mediated changes are quite similar from solar and CO_2 forcing. We also stress, that in Equation 1, we wrote the total cloud change as the sum of the temperature mediated change and adjustment (as well as some contribution from internal variability), but in fact the total cloud change (at any point in time) is not given by the sum of the adjustment (calculated with fixed-SST simulations or our *estimated adjustment* method), and the temperature mediated cloud changes shown in Part I (calculated as a linear fit between cloud changes and global mean surface temperature after year 10). This is because the cloud response is not a linear function of global mean surface temperature (especially in the first 10 years) and consequently the intercept (obtained when calculating the temperature mediated slope) is not the same as the adjustment (see **Supplemental Materials**). Hence, neither the temperature mediated changes presented in Part I nor the adjustments presented here in Part II characterize the non-linear cloud changes that occur (especially during the first ten years).

One might argue that cloud adjustments should be defined as the changes in clouds that are a direct result of the forcing agent on the atmosphere with no change in the surface temperature, including changes in surface temperature pattern (not just the global mean temperature), perhaps following Andrews et al. (2021a). And in this sense, one can simply view the difference between the fixed-surface temperature (“Fixed-Ts”) and “fixed-SST” (or our *estimated adjustment*) as an error or limitation in the calculation of the adjustment (due to land warming) – and at a practical level that is what we have done in this article. But if so, this still leaves us with the problem of characterizing and understanding the non-linear changes that occur as the surface and oceans warm at different rates. From a radiative perspective and at least on the global scale, one can view the situation as one in which there is time-varying radiative feedback (e.g. Knutti & Rugenstein, 2015; Rugenstein & Armour, 2021; Williams et al., 2008) or following the arguments of Rugenstein et al. (2016), a time-varying forcing. Given a sufficiently large ensemble of simulations (which would be used to mitigate the impact of internal variability), it might be possible to extend this to local cloud response. One could use a piecewise linear model to approximate the cloud response to global mean surface temperature such that the slope in the first 10 years can differ from that between years 10 to 150, and we leave such as a possible area of future research. But it seems likely to us that, much as SST patterns have been found to influence the slope of the temperature mediated response on long time scales (e.g. Andrews et al., 2015; Armour, 2017; Rugenstein et al., 2020), variations in both land and sea-surface temperature patterns are likely to have a large effect on the cloud response at shorter time scales; suggesting that it might be better to focus on a unified approach which characterizes the evolution of land and sea-surface temperature, and the impact the patters of land and sea-surface temperature have on clouds.

5. <u>Conclusions</u>

A set of model experiments were requested by CFMIP to allow comparison between the climate response to changes in solar forcing and CO_2 concentrations. In Part I to this paper (Aerenson & Marchand, 2023), we examine the temperature mediated cloud changes from a 4% increase in solar intensity (solp4p) and quadrupling of CO_2 (4xCO2); and in Part II (this paper) we have focused on cloud adjustments – that is the changes in clouds that are a direct result of the forcing agent on the atmosphere which nominally have no influence from change in mean global surface temperature (or perhaps even the surface temperature pattern). Nonetheless, we calculated the 4xCO2 adjustments in the “standard way” using fixed SST simulations (which do allow land surface temperature to increase and do not hold global mean surface temperature fixed) and the calculation for the solp4p adjustment (our new approach, see Section 2) also allows a change in the global pattern of SST. We discuss this situation in more detail in Section 4.4 and raise this issue in this concluding section primarily to stress that the surface temperature changes do have a significant effect on the cloud adjustments presented here. For the remainder of this section, we discuss how temperature medicated and cloud adjustment differ, and address the question "How important are cloud adjustment relative to the temperature mediated feedback?"

As regards the differences between solar and CO_2 cloud responses, in Part I we find that the only notable difference between the temperature mediated cloud changes in solp4p and 4xCO2 is the low cloud fraction change, where there is a greater reduction of low-clouds in the temperature mediated response to solp4p than 4xCO2. In Part II, we find that there are also noteworthy differences in the low and mid-level cloud adjustment to solar and CO_2 forcing. While a variety of mechanisms contribute to these low and mid-level cloud differences, two mechanisms appear to drive much of the differences between the two forcing experiments: 1) Firstly, there is a large mid-level cloud reduction in the adjustment to 4xCO2 due to *the radiative effect* of CO_2 on cloud-top cooling, which is not present in the solp4p experiment (because the increase in solar forcing does not reduce cloud-top cooling to the same extent). 2) Secondly, there are differences in the pattern of surface temperature change. In the solp4p experiment there is more warming in the tropics and subtropics than in the 4xCO2 experiment in both the temperature mediated cloud response and in the adjustment. The enhanced warming in the tropics and subtropics of solp4p (as compared with 4xCO2) causes a stronger low cloud feedback via *the thermodynamic effect*. In Part I, we find *the thermodynamic effect* to be the most important mechanism driving the temperature mediated change of low clouds in the tropics and subtropics. Overall, the differences in adjustments (between solp4p and 4xCO2) have a larger radiative effect than the differences in the temperature mediated cloud changes. The NET cloud feedback parameters for solp4p and 4xCO2 are 0.87 and 0.82 $W/m^2/K$ respectively, which is well within 10% of one another. Meanwhile the NET cloud radiative adjustments (which can be thought of as the cloud contribution to the effective radiative forcing) have a much greater difference between the solp4p and 4xCO2: 0.37 and 0.86 W/m^2 for solp4p and 4xCO2, respectively, in the multi-model mean..

To demonstrate the relative importance of the adjustment and temperature mediated effect during the simulations we show in **Table 2** the change in global mean total NET cloud radiative anomaly averaged over the first and last twenty years of the solp4p and 4xCO2 simulations (where the pre-industrial average has been subtracted), and in parentheses we show the *ratio* of the adjustment to the total cloud change at each time period, as $\frac{Adjustment}{Total\ Anomaly}$. As previously mentioned in Section 3.2, MRI-ESM2-0 produces a strong negative radiative adjustment to solp4p associated with an increase in mid-level clouds (such that the mid-level CF component of the radiative adjustment is negative), which does not occur in the other models, where the adjustments and temperature mediated cloud changes both result in a positive NET radiative effect. As such, this model is excluded from the multi-model mean *ratio* calculation.

Model	Cloud Radiative Anomaly (W/m^2)			
	Abrupt-4xCO2		Abrupt-solp4p	
	Years 0-20	Years 130-150	Years 0-20	Years 130-150
IPSL-CM6A-LR	1.6 (0.47)	3.0 (0.25)	1.0 (1.1)	3.7 (0.29)
MRI-ESM2-0	0.67 (0.80)	1.9 (0.30)	-0.80 (1.23) *	0.27 (-3.56) *
CanESM5	3.6 (0.29)	6.8 (0.15)	3.0 (0.47)	7.4 (0.18)
HadGEM3-GC31-LL	3.5 (0.33)	6.6 (0.17)	2.1 (0.03)	5.7 (0.01)
MM mean	2.3 (0.37)	4.6 (0.19)	1.3 (0.41)	4.3 (0.15)

Table 2 *Global mean NET cloud radiative anomaly averaged over the first and last 20 years of the solp4p and 4xCO2 simulations. In parentheses is the ratio of the adjustment to the total anomaly averaged over each time. The adjustment to solp4p in MRI-ESM2-0 (denoted by asterisks) is negative, while the temperature mediated changes are positive resulting in the total radiative anomaly nearing (and crossing) zero during the simulation. As such the ratio for this simulation becomes spuriously large (and negative) so is excluded from the multi-model mean ratio calculation.*

In the multi-model mean, the adjustment accounts for roughly 40% of the total cloud radiative anomaly in both the solp4p and 4xCO2 in the first 20 years following the abrupt forcing at the end of the simulations the *ratio* has reduced to 19% and 15% for the 4xCO2 and solp4p respectively. There is considerable inter-model spread in the *ratio* with the adjustment being most important (excluding the MRI-ESM2-0 solp4p simulation) in the 4xCO2 from MRI-ESM2-0, in large measure because the temperature mediated changes are small in this model. The cloud radiative adjustment is least important in the solp4p from HadGEM3-GC31-LL, which has a small global mean NET adjustment (see **Figure 4**). This is not to suggest that cloud adjustments are unimportant in this model, because this small global mean NET effect is due to significant LW and SW adjustments which are counter-acting such that the NET is small. As expected, comparing years 0-20 with years 130-150 there is significant reduction in the *ratio* during each model simulation (because cloud radiative effect of the temperature mediated changes becomes larger as the surface temperature increases). So at the end of the simulations the cloud adjustments are less important than the temperature mediated cloud changes, but remain a significant contributor to the overall radiative effect.

Clearly, if we hope to understand future warming both in the near and longer term, understanding and accurately simulating the adjustments, and more generally cloud responses in the first decade (or so) following forcing will be important. Based on our findings and the limiations of the methods used in this study, in our view the community needs to move toward some approach that does not focus only on adjustment (based on fixed-SST simulations) and temperature mediated (linear slope) response in later years, and perhaps characterizes the temporal evolution of land and sea-surface temperature changes and the associated cloud response over multiple timescales, including the first decade or so following the forcing change.

Acknowledgments

This research was supported by the MISR project at the NASA Jet Propulsion Laboratory (under contract no. 1318945). The authors wish to acknowledge and thank the many modelling centers who contributed data to the Coupled Model Intercomparison Project that was necessary for this study.

Open Research

All CMIP6 data used in this study are available for downlowad from the World Climate Research Program (WCRP) CMIP6 data archive (https://esgf-node.llnl.gov/search/cmip6/). The model simulations used to validate the *estimated* adjustment method from CESM1 are available for download at https://doi.org/10.5281/zenodo.7193943, and details on accessing the data from the PDRMIP simulations is provided at https://cicero.oslo.no/en/projects/pdrmip/pdrmip-data-access. Additionally the cloud radiative kernels were downloaded from https://github.com/mzelinka.

References

Aerenson, T., Marchand, R. (2023). Cloud Response to Abrupt Solar and CO2 Forcing Part I: Temperature Mediated Cloud Feedbacks

Andrews, T., Bodas-Salcedo, A., Gregory, J. M., Dong, Y., Armour, K. C., Paynter, D., Lin, P., Modak, A., Mauritsen, T., Cole, J. N. S., Medeiros, B., Benedict, J. J., Douville, H., Roehrig, R., Koshiro, T., Kawai, H., Ogura, T., Dufresne, J. L., Allan, R. P., & Liu, C. (2022). On the Effect of Historical SST Patterns on Radiative Feedback. *Journal of Geophysical Research: Atmospheres*, *127*(18), e2022JD036675. https://doi.org/10.1029/2022JD036675

Andrews, T., Boucher, O., Fläschner, D., Kasoar, M., Kharin, V. V., Kirkevåg, A., Lamarque, J.-F., Myhre, G., Mülmenstädt, J., Oliviè, D. J. L., Samset, B. H., Sandstad, M., Shawki, D., & Shinde, D. (2021b). Precipitation Driver Response Model Intercomparison Project data sets 2013-2021. *World Data Center for Climate (WDCC) at DKRZ.*

Andrews, T., Gregory, J. M., & Webb, M. J. (2015). The dependence of radiative forcing and feedback on evolving patterns of surface temperature change in climate models. *Journal of Climate*, *28*(4), 1630–1648. https://doi.org/10.1175/JCLI-D-14-00545.1

Andrews, T., Smith, C. J., Myhre, G., Forster, P. M., Chadwick, R., & Ackerley, D. (2021a). Effective Radiative Forcing in a GCM With Fixed Surface Temperatures. *Journal of Geophysical Research: Atmospheres*, *126*(4), e2020JD033880. https://doi.org/10.1029/2020JD033880

Armour, K. C. (2017). Energy budget constraints on climate sensitivity in light of inconstant climate feedbacks. *Nature Climate Change*, *7*(5), 331–335. https://doi.org/10.1038/nclimate3278

Betts, R. A., Cox, P. M., Lee, S. E., & Woodward, F. I. (1997). Contrasting physiological and structural vegetation feedbacks in climate change simulations. *Nature 1997 387:6635*, *387*(6635), 796–799. https://doi.org/10.1038/42924

Bodas-Salcedo, A., Webb, M. J., Bony, S., Chepfer, H., Dufresne, J. L., Klein, S. A., Zhang, Y., Marchand, R., Haynes, J. M., Pincus, R., & John, V. O. (2011). COSP: Satellite simulation software for model assessment. *Bulletin of the American Meteorological Society*, *92*(8), 1023–1043. https://doi.org/10.1175/2011BAMS2856.1

Bretherton, C. S. (2015). Insights into low-latitude cloud feedbacks from high-resolution models. In *Philosophical Transactions of the Royal Society A: Mathematical, Physical and Engineering Sciences* (Vol. 373, Issue 2054). The Royal Society Publishing. https://doi.org/10.1098/rsta.2014.0415

Bretherton, C. S., & Smolarkiewicz, P. K. (1989). Gravity waves, compensating subsidence and detrainment around cumulus clouds. *Journal of the Amospheric Sciences*, *46*(6), 740–759. https://doi.org/10.1175/1520-0469(1989)046<0740:GWCSAD>2.0.CO;2

Ceppi, P., Brient, F., Zelinka, M. D., & Hartmann, D. L. (2017). Cloud feedback mechanisms and their representation in global climate models. In *Wiley Interdisciplinary Reviews: Climate Change* (Vol. 8, Issue 4, p. 465). https://doi.org/10.1002/wcc.465

Chadwick, R., Ackerley, D., Ogura, T., & Dommenget, D. (2019). Separating the Influences of Land Warming, the Direct CO 2 Effect, the Plant Physiological Effect, and SST Warming on Regional Precipitation Changes. *Journal of Geophysical Research: Atmospheres*, *124*(2), 624–640. https://doi.org/10.1029/2018JD029423

Colman, R. A., & McAvaney, B. J. (2011). On tropospheric adjustment to forcing and climate feedbacks. *Climate Dynamics*, *36*(9–10), 1649–1658. https://doi.org/10.1007/s00382-011-1067-4

Cox, P. M., Betts, R. A., Bunton, C. B., Essery, R. L. H., Rowntree, P. R., & Smith, J. (1999). The impact of new land surface physics on the GCM simulation of climate and climate sensitivity. *Climate Dynamics*, *15*(3), 183–203. https://doi.org/10.1007/S003820050276/METRICS

Dinh, T. P., Durran, D. R., & Ackerman, T. P. (2010). Maintenance of tropical tropopause layer cirrus. *Journal of Geophysical Research Atmospheres*, *115*(D2). https://doi.org/10.1029/2009JD012735

Eyring, V., Bony, S., Meehl, G. A., Senior, C. A., Stevens, B., Stouffer, R. J., & Taylor, K. E. (2016). Overview of the Coupled Model Intercomparison Project Phase 6 (CMIP6) experimental design and organization. *Geoscientific Model Development*, *9*(5), 1937–1958. https://doi.org/10.5194/gmd-9-1937-2016

Field, C. B., Jackson, R. B., & Mooney, H. A. (1995). Stomatal responses to increased CO2: implications from the plant to the global scale. *Plant, Cell & Environment*, *18*(10), 1214–1225. https://doi.org/10.1111/J.1365-3040.1995.TB00630.X

Forster, P. M., Richardson, T., Maycock, A. C., Smith, C. J., Samset, B. H., Myhre, G., Andrews, T., Pincus, R., & Schulz, M. (2016). Recommendations for diagnosing effective radiative forcing from climate models for CMIP6. *Journal of Geophysical Research*, *121*(20), 12,460-12,475. https://doi.org/10.1002/2016JD025320

Gasparini, B., Blossey, P. N., Hartmann, D. L., Lin, G., & Fan, J. (2019). What Drives the Life Cycle of Tropical Anvil Clouds? *Journal of Advances in Modeling Earth Systems*, *11*(8), 2586–2605. https://doi.org/10.1029/2019MS001736

Gates, W. L., Boyle, J. S., Covey, C., Dease, C. G., Doutriaux, C. M., Drach, R. S., Fiorino, M., Gleckler, P. J., Hnilo, J. J., Marlais, S. M., Phillips, T. J., Potter, G. L., Santer, B. D., Sperber, K. R., Taylor, K. E., & Williams, D. N. (1999). An Overview of the Results of the Atmospheric Model Intercomparison Project (AMIP I). In *Bulletin of the American Meteorological Society* (Vol. 80, Issue 1, pp. 29–55). https://doi.org/10.1175/1520-0477(1999)080<0029:AOOTRO>2.0.CO;2

Gregory, J. M., Ingram, W. J., Palmer, M. A., Jones, G. S., Stott, P. A., Thorpe, R. B., Lowe, J. A., Johns, T. C., & Williams, K. D. (2004). A new method for diagnosing radiative forcing and climate sensitivity. *Geophysical Research Letters*, *31*(3). https://doi.org/10.1029/2003GL018747

Gregory, J. M., & Webb, M. (2008). Tropospheric adjustment induces a cloud component in CO2 forcing. *Journal of Climate*, *21*(1), 58–71. https://doi.org/10.1175/2007JCLI1834.1

Immler, F., Krüger, K., Fujiwara, M., Verver, G., Rex, M., & Schrems, O. (2008). Correlation between equatorial Kelvin waves and the occurrence of extremely thin ice clouds at the tropical tropopause. *Atmospheric Chemistry and Physics*, *8*(14), 4019–4026. https://doi.org/10.5194/ACP-8-4019-2008

Kamae, Y., Chadwick, R., Ackerley, D., Ringer, M., & Ogura, T. (2019). Seasonally variant low cloud adjustment over cool oceans. *Climate Dynamics*, *52*(9–10), 5801–5817. https://doi.org/10.1007/S00382-018-4478-7/FIGURES/12

Kaur, H., Bala, G., Seshadri, A. K., & Sciences, O. (2023). Why is Climate Sensitivity for Solar Forcing less than for an Equivalent. *Journal of Climate*, *36*(3), 1–39. https://doi.org/10.1175/JCLI-D-21-0980.1

Knutti, R., & Rugenstein, M. A. A. (2015). Feedbacks, climate sensitivity and the limits of linear models. *Philosophical Transactions of the Royal Society A: Mathematical, Physical and Engineering Sciences*, *373*(2054). https://doi.org/10.1098/RSTA.2015.0146

Kravitz, B., Robock, A., Tilmes, S., Boucher, O., English, J. M., Irvine, P. J., Jones, A., Lawrence, M. G., MacCracken, M., Muri, H., Moore, J. C., Niemeier, U., Phipps, S. J., Sillmann, J., Storelvmo, T., Wang, H., & Watanabe, S. (2015). The Geoengineering Model Intercomparison Project Phase 6 (GeoMIP6): Simulation design and preliminary results. *Geoscientific Model Development*, *8*(10), 3379–3392. https://doi.org/10.5194/gmd-8-3379-2015

Larson, E. J. L., & Portmann, R. W. (2016). A temporal kernel method to compute effective radiative forcing in CMIP5 transient simulations. *Journal of Climate*, *29*(4), 1497–1509. https://doi.org/10.1175/JCLI-D-15-0577.1

Mapes, B. E. (1993). Gregarious tropical convection. *Journal of the Atmospheric Sciences*, *50*(13), 2026–2037. https://doi.org/10.1175/1520-0469(1993)050<2026:GTC>2.0.CO;2

Mercado, L. M., Bellouin, N., Sitch, S., Boucher, O., Huntingford, C., Wild, M., & Cox, P. M. (2009). Impact of changes in diffuse radiation on the global land carbon sink. *Nature 2009 458:7241*, *458*(7241), 1014–1017. https://doi.org/10.1038/nature07949

Modak, A., Bala, G., Cao, L., & Caldeira, K. (2016). Why must a solar forcing be larger than a CO2 forcing to cause the same global mean surface temperature change? *Environmental Research Letters*, *11*(4), 044013. https://doi.org/10.1088/1748-9326/11/4/044013

Myhre, G., Forster, P. M., Samset, B. H., Hodnebrog, Sillmann, J., Aalbergsjø, S. G., Andrews, T., Boucher, O., Faluvegi, G., Fläschner, D., Iversen, T., Kasoar, M., Kharin, V., Kirkevag, A., Lamarque, J. F., Olivié, D., Richardson, T. B., Shindell, D., Shine, K. P., … Zwiers, F. (2017). PDRMIP: A precipitation driver and response model intercomparison project-protocol and preliminary results. *Bulletin of the American Meteorological Society*, *98*(6), 1185–1198. https://doi.org/10.1175/BAMS-D-16-0019.1

Myhre, G., Samset, B., Forster, P. M., Hodnebrog, Ø., Sandstad, M., Mohr, C. W., Sillmann, J., Stjern, C. W., Andrews, T., Boucher, O., Faluvegi, G., Iversen, T., Lamarque, J. F., Kasoar, M., Kirkevåg, A., Kramer, R., Liu, L., Mülmenstädt, J., Olivié, D., … Watson-Parris, D. (2022). Scientific data from precipitation driver response model intercomparison project. *Scientific Data*, *9*(1), 1–7. https://doi.org/10.1038/s41597-022-01194-9

Neale, R., Chen, C., Gettelman, A., Lauritzen, P., Park, S., Williamson, D., Conley, A., Garcia, R., Kinnison, D., Lamarque, J., Marsh, D., Mills, M., Smith, A., Tilmes, S., Vitt, F., Morrison, H., Cameron-Smith, P., Collins, W., Iacono, M., … Taylor, M. (2012). Description of the NCAR community atmosphere model (CAM 5.0), NCAR technical note. *Boulder, Colo: NCAR TN (486)*, *486*.

Qu, X., Hall, A., Klein, S. A., & Caldwell, P. M. (2014). On the spread of changes in marine low cloud cover in climate model simulations of the 21st century. *Climate Dynamics*, *42*(9–10), 2603–2626. https://doi.org/10.1007/s00382-013-1945-z

Rossow, W. B., & Schiffer, R. A. (1991). ISCCP cloud data products. *Bulletin - American Meteorological Society*, *72*(1), 2–20. https://doi.org/10.1175/1520-0477(1991)072<0002:ICDP>2.0.CO;2

Rugenstein, M. A. A., & Armour, K. C. (2021). Three Flavors of Radiative Feedbacks and Their Implications for Estimating Equilibrium Climate Sensitivity. *Geophysical Research Letters*, *48*(15), e2021GL092983. https://doi.org/10.1029/2021GL092983

Rugenstein, M. A. A., Gregory, J. M., Schaller, N., Sedlácek, J., & Knutti, R. (2016). Multiannual ocean-atmosphere adjustments to radiative forcing. *Journal of Climate*, *29*(15), 5643–5659. https://doi.org/10.1175/JCLI-D-16-0312.1

Rugenstein, M., Bloch-Johnson, J., Gregory, J., Andrews, T., Mauritsen, T., Li, C., Frölicher, T. L., Paynter, D., Danabasoglu, G., Yang, S., Dufresne, J. L., Cao, L., Schmidt, G. A., Abe-Ouchi, A., Geoffroy, O., & Knutti, R. (2020). Equilibrium Climate Sensitivity Estimated by Equilibrating Climate Models. *Geophysical Research Letters*, *47*(4). https://doi.org/10.1029/2019GL083898

Russotto, R. D., & Ackerman, T. P. (2018). Changes in clouds and thermodynamics under solar geoengineering and implications for required solar reduction. *Atmospheric Chemistry and Physics*, *18*(16), 11905–11925. https://doi.org/10.5194/acp-18-11905-2018

Salvi, P., Ceppi, P., & Gregory, J. M. (2021). Interpreting the Dependence of Cloud-Radiative Adjustment on Forcing Agent. *Geophysical Research Letters*, *48*(18), e2021GL093616. https://doi.org/10.1029/2021GL093616

Schneider, T., Kaul, C. M., & Pressel, K. G. (2019). Possible climate transitions from breakup of stratocumulus decks under greenhouse warming. *Nature Geoscience*, *12*(3), 164–168. https://doi.org/10.1038/s41561-019-0310-1

Seeley, J. T., Jeevanjee, N., Langhans, W., & Romps, D. M. (2019). Formation of Tropical Anvil Clouds by Slow Evaporation. *Geophysical Research Letters*, *46*(1), 492–501. https://doi.org/10.1029/2018GL080747

Sherwood, S. C., Bony, S., Boucher, O., Bretherton, C., Forster, P. M., Gregory, J. M., & Stevens, B. (2015). Adjustments in the forcing-feedback framework for understanding climate change. *Bulletin of the American Meteorological Society*, *96*(2), 217–228. https://doi.org/10.1175/BAMS-D-13-00167.1

Sherwood, S. C., Webb, M. J., Annan, J. D., Armour, K. C., Forster, P. M., Hargreaves, J. C., Hegerl, G., Klein, S. A., Marvel, K. D., Rohling, E. J., Watanabe, M., Andrews, T., Braconnot, P., Bretherton, C. S., Foster, G. L., Hausfather, Z., von der Heydt, A. S., Knutti, R., Mauritsen, T., … Zelinka, M. D. (2020). An Assessment of Earth's Climate Sensitivity Using Multiple Lines of Evidence. In *Reviews of Geophysics* (Vol. 58, Issue 4). Blackwell Publishing Ltd. https://doi.org/10.1029/2019RG000678

Smith, C. J., Kramer, R. J., Myhre, G., Forster, P. M., Soden, B. J., Andrews, T., Boucher, O., Faluvegi, G., Fläschner, D., Hodnebrog, Kasoar, M., Kharin, V., Kirkevåg, A., Lamarque, J. F., Mülmenstädt, J., Olivié, D., Richardson, T., Samset, B. H., Shindell, D., … Watson-Parris, D. (2018). Understanding Rapid Adjustments to Diverse Forcing Agents. *Geophysical Research Letters*, *45*(21), 12,023-12,031. https://doi.org/10.1029/2018GL079826

Sobel, A. H., & Bretherton, C. S. (2000). Modeling tropical precipitation in a single column. *Journal of Climate*, *13*(24), 4378–4392. https://doi.org/10.1175/1520-0442(2000)013<4378:MTPIAS>2.0.CO;2

Spichtinger, P., Gierens, K., & Dörnbrack, A. (2005). Formation of ice supersaturation by mesoscale gravity waves. *Atmospheric Chemistry and Physics*, *5*(5), 1243–1255. https://doi.org/10.5194/ACP-5-1243-2005

Su, W., Bodas-Salcedo, A., Xu, K. M., & Charlock, T. P. (2010). Comparison of the tropical radiative flux and cloud radiative effect profiles in a climate model with Clouds and the Earth's Radiant Energy System (CERES) data. *Journal of Geophysical Research Atmospheres*, *115*(1), 1105. https://doi.org/10.1029/2009JD012490

Taylor, K. E., Crucifix, M., Braconnot, P., Hewitt, C. D., Doutriaux, C., Broccoli, A. J., Mitchell, J. F. B., & Webb, M. J. (2007). Estimating shortwave radiative forcing and response in climate models. *Journal of Climate*, *20*(11), 2530–2543. https://doi.org/10.1175/JCLI4143.1

Tselioudis, G., Rossow, William. B., Jakob, C., Remillard, J., Tropf, D., & Zhang, Y. (2021). Evaluation of Clouds, Radiation, and Precipitation in CMIP6 Models Using Global Weather States Derived from ISCCP-H Cloud Property Data. *Journal of Climate*, *34*(17), 1–42. https://doi.org/10.1175/jcli-d-21-0076.1

Webb, M. J., Andrews, T., Bodas-Salcedo, A., Bony, S., Bretherton, C. S., Chadwick, R., Chepfer, H., Douville, H., Good, P., Kay, J. E., Klein, S. A., Marchand, R., Medeiros, B., Pier Siebesma, A., Skinner, C. B., Stevens, B., Tselioudis, G., Tsushima, Y., & Watanabe, M. (2017). The Cloud Feedback Model Intercomparison Project (CFMIP) contribution to CMIP6. *Geoscientific Model Development*, *10*(1), 359–384. https://doi.org/10.5194/gmd-10-359-2017

Williams, K. D., Ingram, W. J., & Gregory, J. M. (2008). Time variation of effective climate sensitivity in GCMs. *Journal of Climate*, *21*(19), 5076–5090. https://doi.org/10.1175/2008JCLI2371.1

Wood, R., & Bretherton, C. S. (2006). On the relationship between stratiform low cloud cover and lower-tropospheric stability. *Journal of Climate*, *19*(24), 6425–6432. https://doi.org/10.1175/JCLI3988.1

Zelinka, M. D., Klein, S. A., & Hartmann, D. L. (2012a). Computing and partitioning cloud feedbacks using cloud property histograms. Part I: Cloud radiative kernels. *Journal of Climate*, *25*(11), 3715–3735. https://doi.org/10.1175/JCLI-D-11-00248.1

Zelinka, M. D., Klein, S. A., & Hartmann, D. L. (2012b). Computing and partitioning cloud feedbacks using cloud property histograms. Part II: Attribution to changes in cloud amount, altitude, and optical depth. *Journal of Climate*, *25*(11), 3736–3754. https://doi.org/10.1175/JCLI-D-11-00249.1

Zelinka, M. D., Klein, S. A., Taylor, K. E., Andrews, T., Webb, M. J., Gregory, J. M., & Forster, P. M. (2013). Contributions of different cloud types to feedbacks and rapid adjustments in CMIP5. *Journal of Climate*, *26*(14), 5007–5027. https://doi.org/10.1175/JCLI-D-12-00555.1

Zelinka, M. D., Myers, T. A., McCoy, D. T., Po-Chedley, S., Caldwell, P. M., Ceppi, P., Klein, S. A., & Taylor, K. E. (2020). Causes of Higher Climate Sensitivity in CMIP6 Models. *Geophysical Research Letters*, *47*(1). https://doi.org/10.1029/2019GL085782

Zelinka, M. D., Tan, I., Oreopoulos, L., & Tselioudis, G. (2022). Detailing cloud property feedbacks with a regime-based decomposition. *Climate Dynamics*, 1–21. https://doi.org/10.1007/s00382-022-06488-7

Zhou, C., Wang, M., Zelinka, M. D., Liu, Y., Dong, Y., & Armour, K. C. (2023). Explaining Forcing Efficacy With Pattern Effect and State Dependence. *Geophysical Research Letters*, *50*(3), 1–9. https://doi.org/10.1029/2022GL101700